

HyspIRI VSWIR Level 2 ATBDs and Sample Science Results from HICO on the International Space Station

Bo-Cai Gao

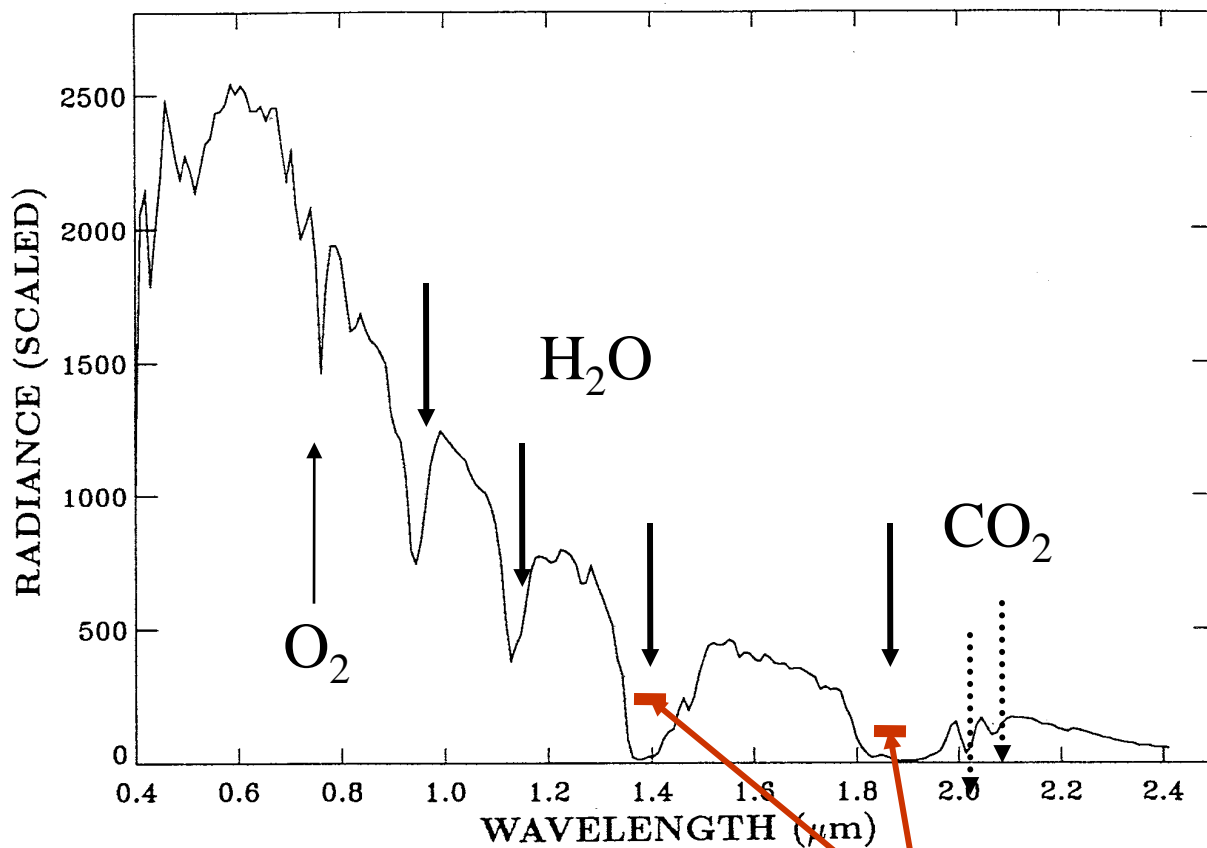
Remote Sensing Division,
Naval Research Laboratory, Washington, DC USA

OUTLINE

- VSWIR Level 2 ATBD for Land Surface Reflectance Retrievals
- VSWIR Level 2 ATBD for Water Leaving Reflectance Retrievals
- Preliminary Science Results from HICO on the International Space Station
- Summary

Atmospheric Correction Over Land

An AVIRIS Spectrum



The AVIRIS spectrum is affected by atmospheric absorption and scattering effects. In order to obtain the surface reflectance spectrum, the atmospheric effects need to be removed.

Strong water vapor bands are located near 1.38 and 1.88 micron. No signals are detected under clear sky conditions.

Equations For Atmospheric Correction Over Land

The measured radiance at the satellite level can be expressed as:

$$L_{\text{obs}} = L_a + L_{\text{sun}} t \rho \quad (1)$$

L_a : path radiance;

ρ : surface reflectance;

L_{sun} : solar radiance above the atmosphere;

t : *2-way transmittance for the Sun-surface-sensor path*

Define the satellite apparent reflectance as

$$\rho_{\text{obs}}^* = \pi L_{\text{obs}} / (\mu_0 E_0) \quad (2)$$

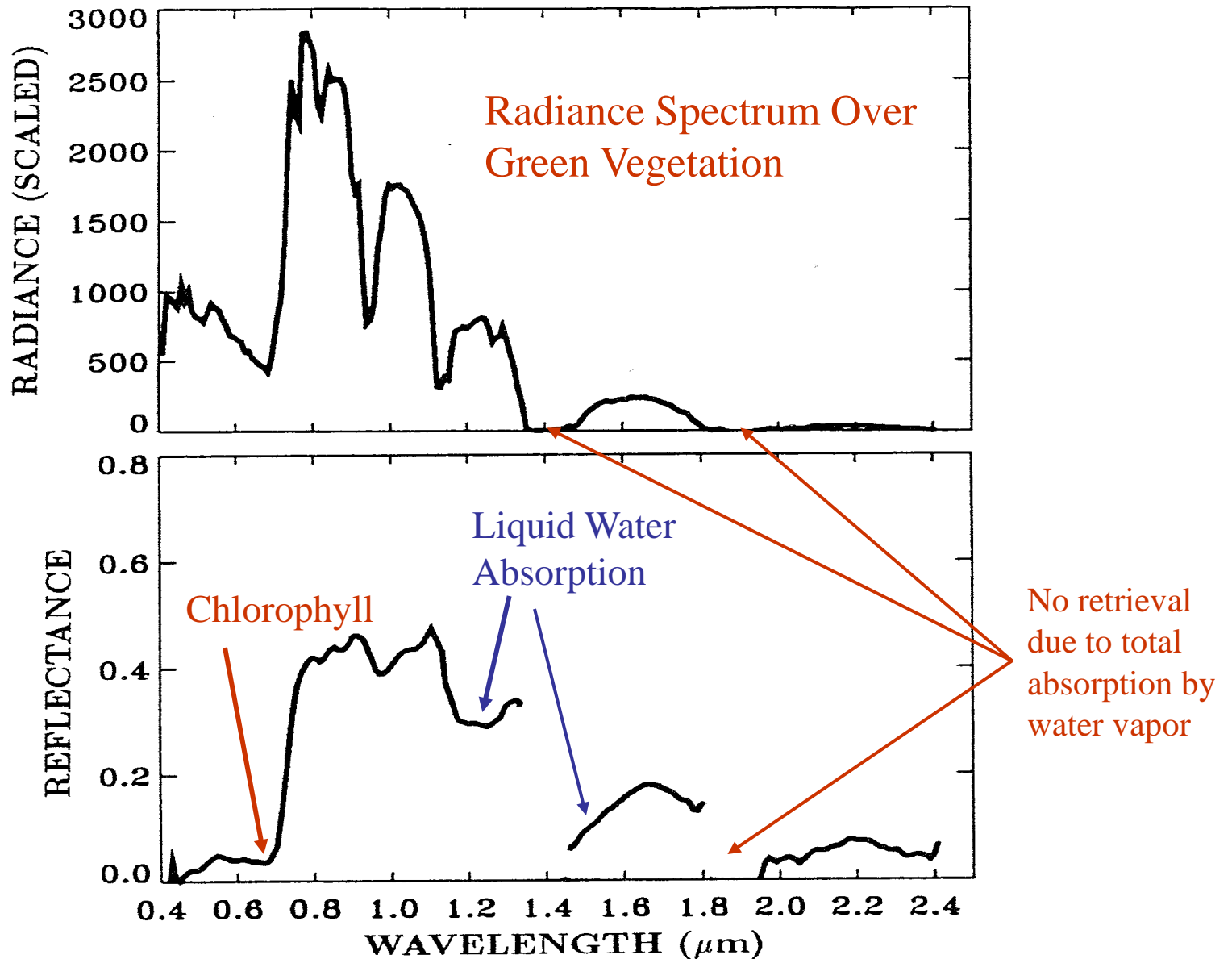
$$\rho_{\text{obs}}^* = T_g [\rho_a + t \rho / (1 - \rho s)] \quad (3)$$

By inverting Eq. (3) for ρ , we get:

$$\rho = (\rho_{\text{obs}}^* / T_g - \rho_a^*) / [t + s (\rho_{\text{obs}}^* / T_g - \rho_a^*)] \quad (4)$$

Gao, B.-C., K. H. Heidebrecht, and A. F. H. Goetz, Derivation of scaled surface reflectances from AVIRIS data, *Remote Sens. Env.*, 44, 165-178, 1993.

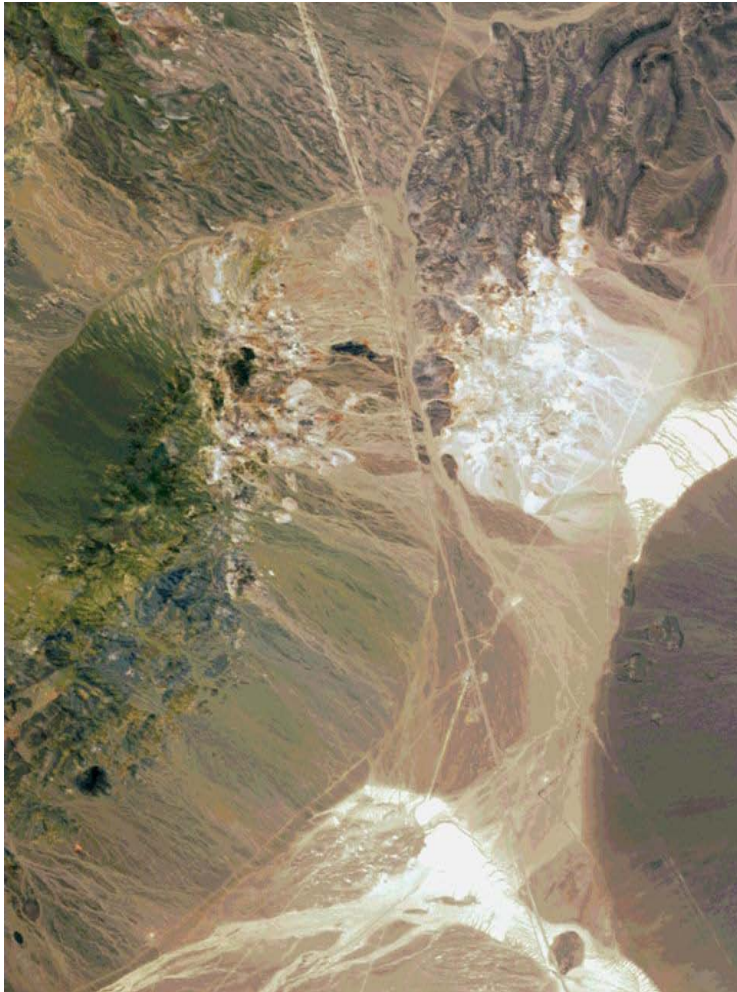
SAMPLE REFLECTANCE RETRIEVALS WITH ATREM



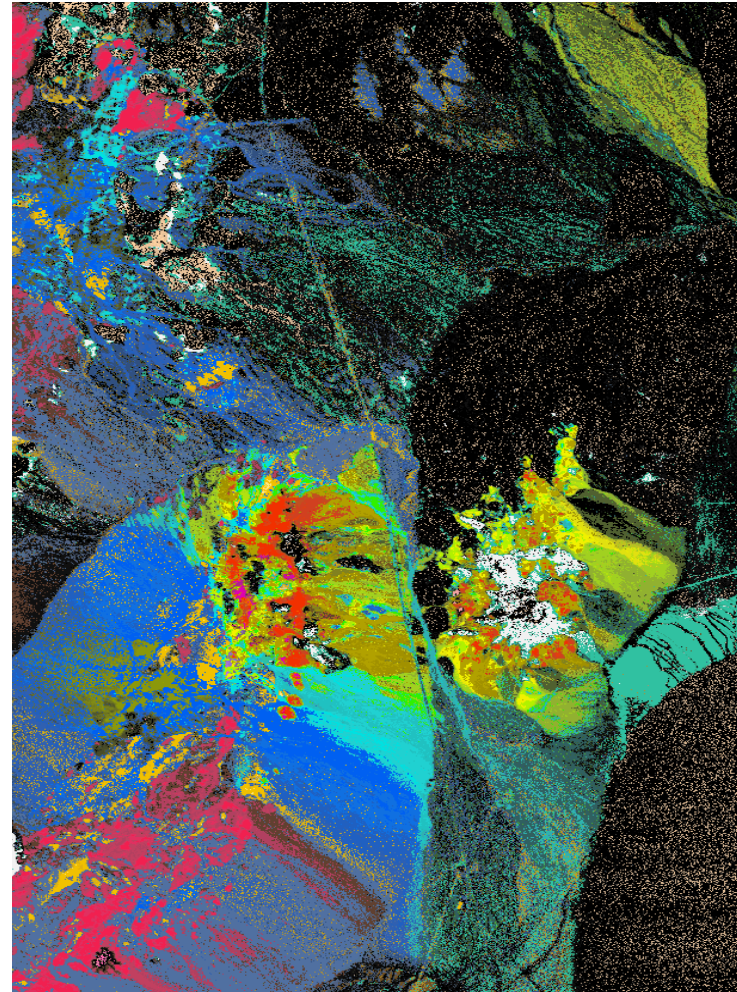
MINERAL MAPPING USING ATREM OUTPUT

by Scientists at USGS in Denver, Colorado

RGB Image (Cuprite, NV)



USGS Mineral Map, ~11x18 km



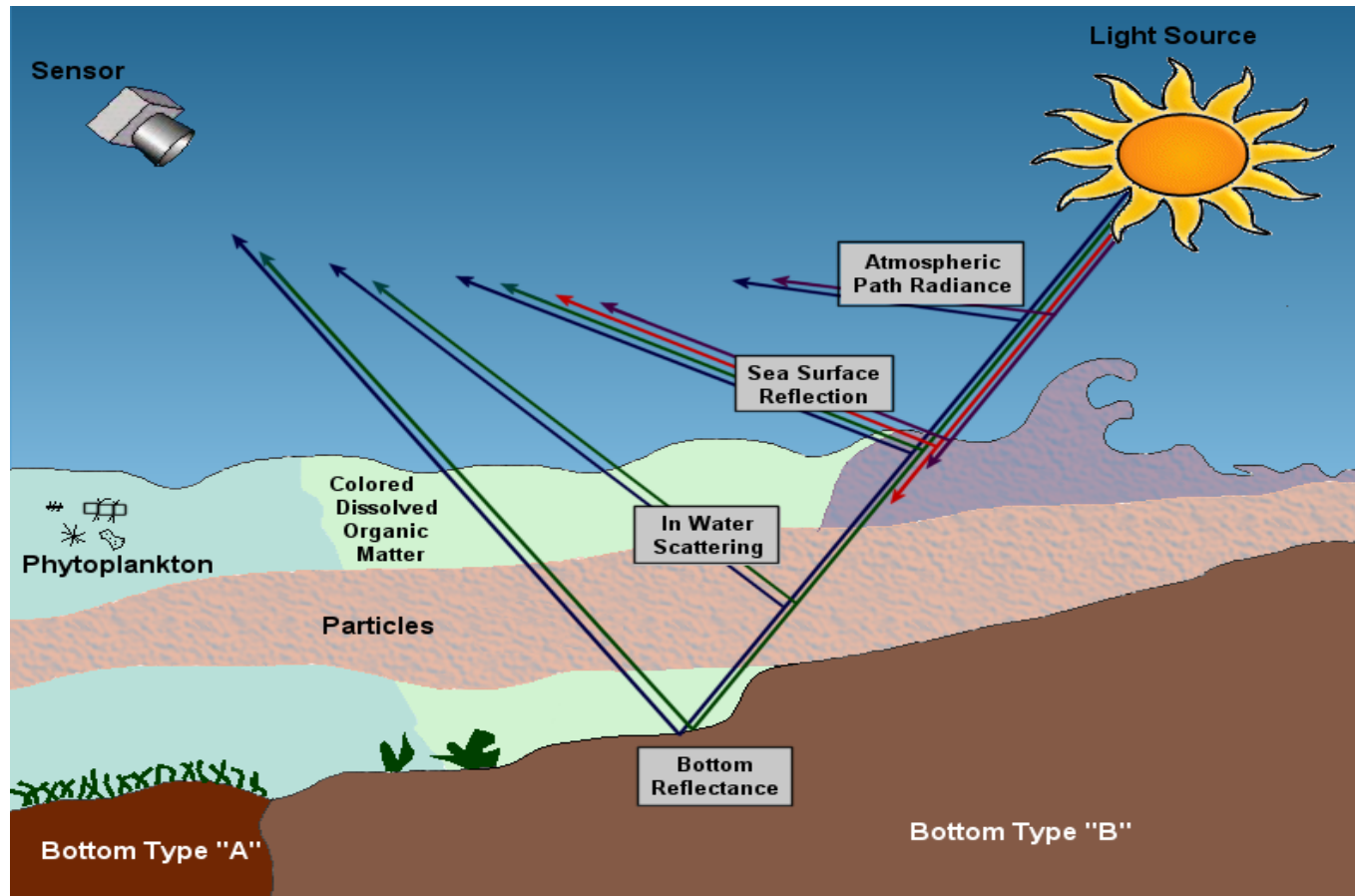
Cuprite, Nevada
 AVIRIS 1995 Data
 USGS
 Clark & Swayze
 Tricorder 3.3 product

Red	K-Alunite 150C
Orange	K-Alunite 250C
Light Orange	K-Alunite 450C
Pink	Na ₈ 2-Alunite 100C
Magenta	Na ₄ 0-Alunite 400C
Yellow	Kaolinite wx1
Light Green	Kaolinite px1
Cyan	Kaolinite+smectite or muscovite
Bright Green	Halloysite
Purple	Dickite
Olive Green	Alunite+Kaolinite and/or Muscovite
Red	Calcite
Dark Blue	Calcite + Montmorillonite
Light Blue	Calcite +Kaolinite
Teal	Na- Montmorillonite
Yellow	low-Al muscovite
Orange	med-Al muscovite
Blue	high-Al muscovite
Light Blue	Jarosite
Pink	Buddingtonite
White	Chalcedony
Light Orange	Nontronite
Light Green	Pyrophyllite + alunite
Dark Green	Chlorite + Montmorillonite or Muscovite
Magenta	Chlorite

2 km

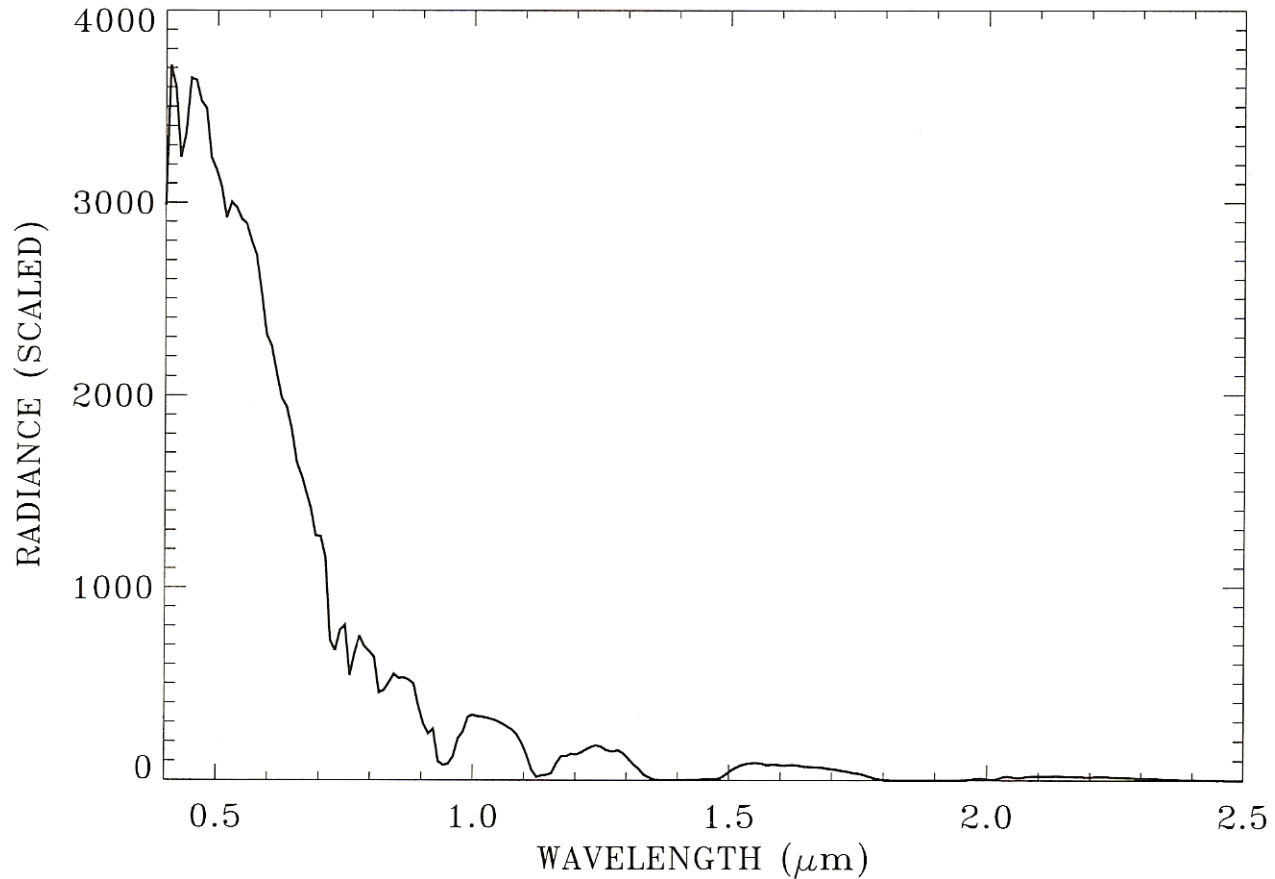
N

Atmospheric Correction Over Water



Over the dark water surfaces, ~90% of satellite radiances come from the atmosphere, and ~10% come from water. Very accurate atmospheric corrections are required in order to derive the useful water leaving reflectances. The specular reflection at the air/water interface introduces additional complications for modeling.

An AVIRIS Spectrum Over A Water Pixel



The radiances above one micron are very small.

Relevant Equations and Definitions

In the absence of gas absorption, the radiance at the satellite level is:

$$L_{obs} = L_0 + L_{sfc} t'_u + L_w t_u, \quad (1)$$

L_0 : path radiance; L_w : water leaving radiance;

L_{sfc} : radiance reflected at water surface; t_u : upward transmittance

Define
$$L_{atm+sfc} = L_0 + L_{sfc} t'_u \quad (2)$$

Eq. (1) becomes:
$$L_{obs} = L_{atm+sfc} + L_w t_u \quad (3)$$

Multiply Eq. (3) by π and divide by $(\mu_0 E_0)$, Eq. (3) becomes:

$$\pi L_{obs} / (\mu_0 E_0) = \pi L_{atm+sfc} / (\mu_0 E_0) + \pi L_w t_d t_u / (\mu_0 E_0 t_d) \quad (4)$$

Several reflectances are defined as:

Satellite apparent reflectance:
$$\rho^*_{obs} = \pi L_{obs} / (\mu_0 E_0), \quad (5)$$

$$\rho^*_{atm+sfc} = \pi L_{atm+sfc} / (\mu_0 E_0), \quad (6)$$

Water leaving reflectance:
$$\rho_w = \pi L_w / (\mu_0 E_0 t_d) = \pi L_w / E_d \quad (7)$$

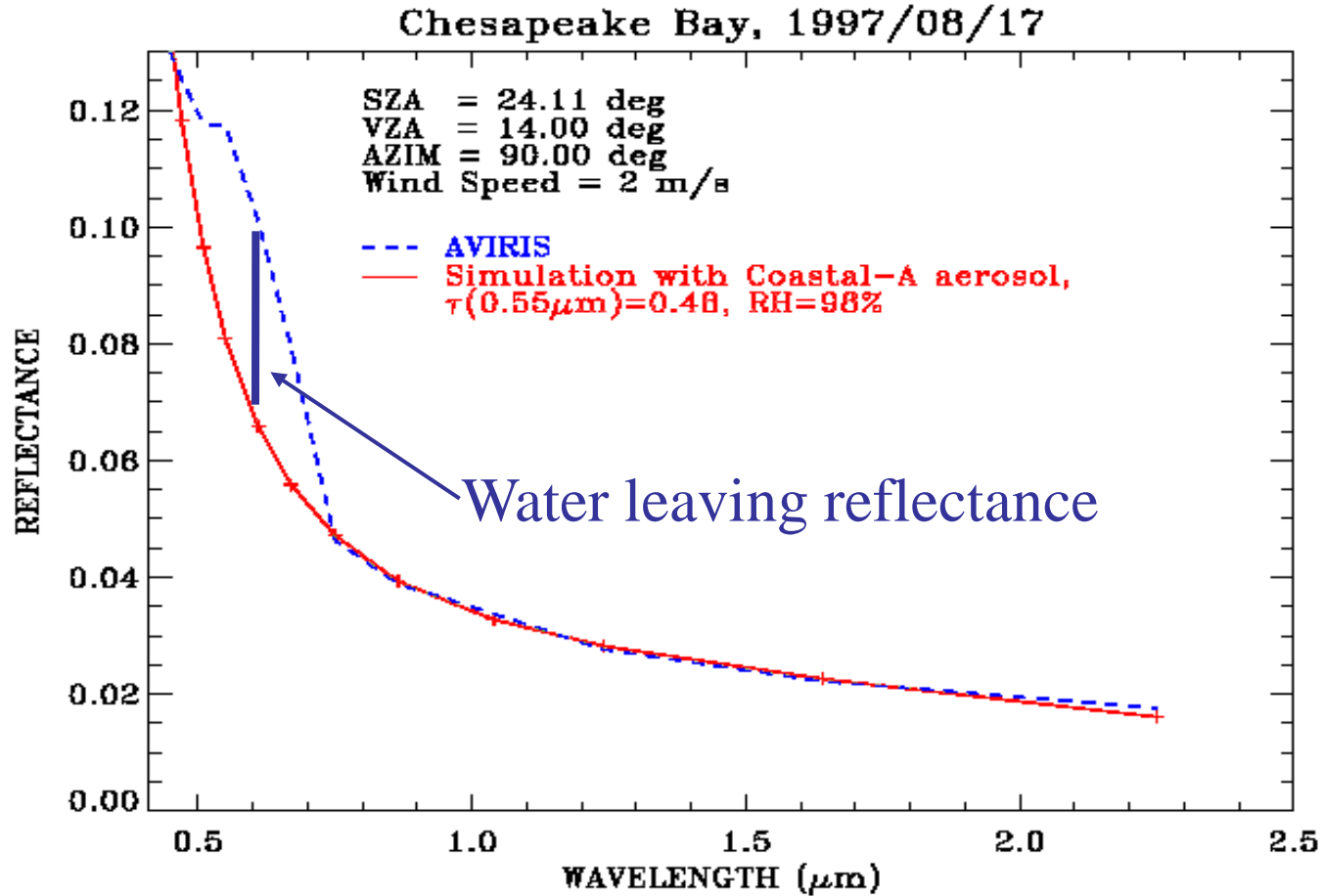
Remote sensing reflectance:
$$R_{rs} = \rho_w / \pi = L_w / E_d \quad (7')$$

Substitute Eqs (5) – (7) into Eq. (4):
$$\rho^*_{obs} = \rho^*_{atm+sfc} + \rho_w t_d t_u \quad (8)$$

After consideration of gas absorption and multiple reflection between the atmosphere and surface and with further manipulation, we can get:

$$\rho_w = (\rho^*_{obs} / T_g - \rho^*_{atm+sfc}) / [t_d t_u + s (\rho^*_{obs} / T_g - \rho^*_{atm+sfc})] \quad (11)$$

Atmospheric Correction for Water Surfaces



Channels at 0.86 and longer wavelengths are used to estimate atmospheric effects, and then extrapolate to the visible region. The differences between the two curves above are proportional to water leaving reflectances.

Glint Removal Using AVIRIS Data Over Kaneohe Bay, HI

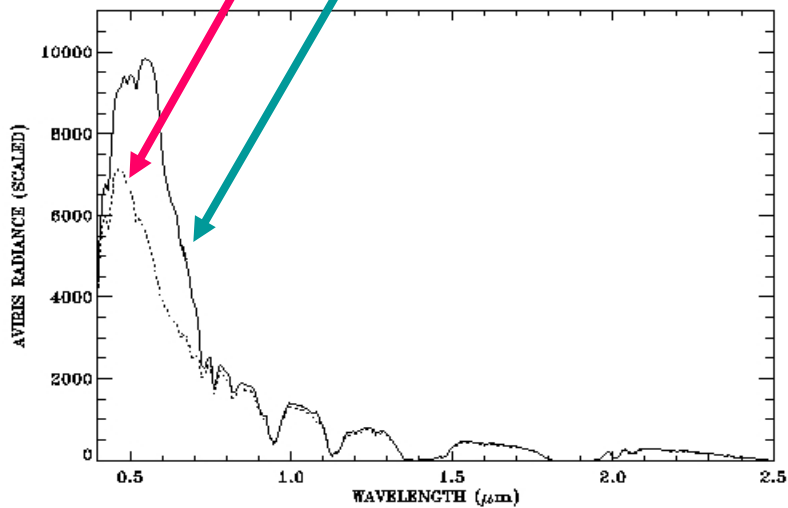
Before



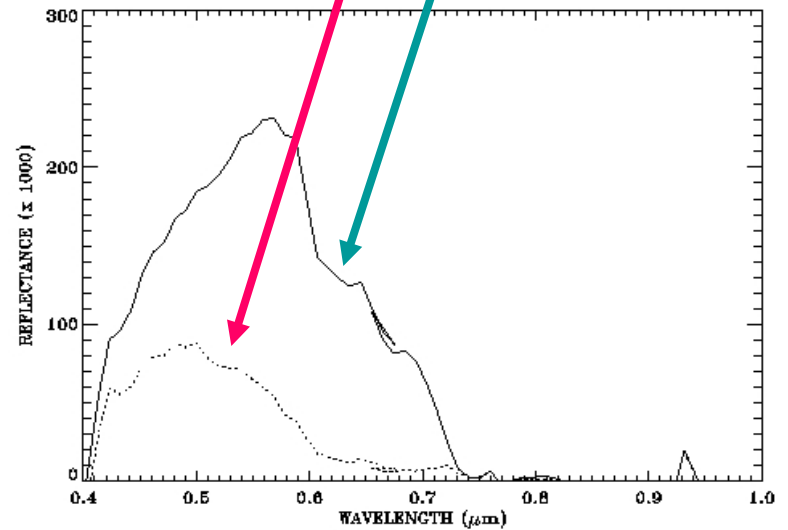
After



Sample Radiance Spectra

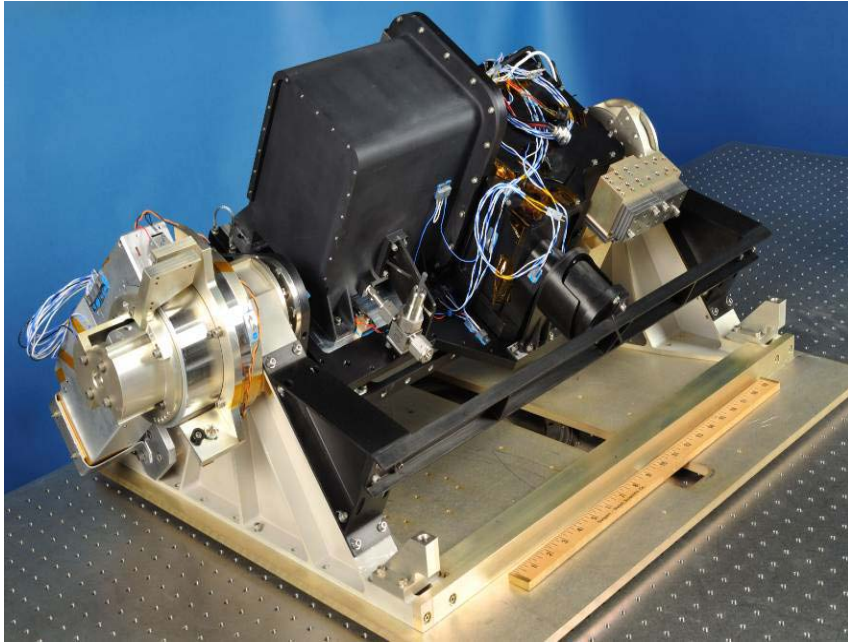


Sample Derived Reflectance Spectra



The HICO Instrument on The International Space Station

HICO as delivered



Optical diagram



Earth Surface Images from HICO

Images are about 43 km wide and 190 km long
Orientations are given below



Cape Town, South Africa, Oct. 3, 2009. Orientation is from NW at top to SE at bottom.



Lower Chesapeake Bay, Oct. 7, 2009. Orientation is from NW at top to SE at bottom.



Coast of South China Sea, near Hong Kong, China, Oct. 2, 2009. Orientation is from SW at bottom to NE at top.



Part of the Grand Canyon, Sept. 27, 2009. The center of the image is at $35^{\circ} 50' N$, $111^{\circ} 23' W$ and the orientation is from SW at bottom to NE at top.



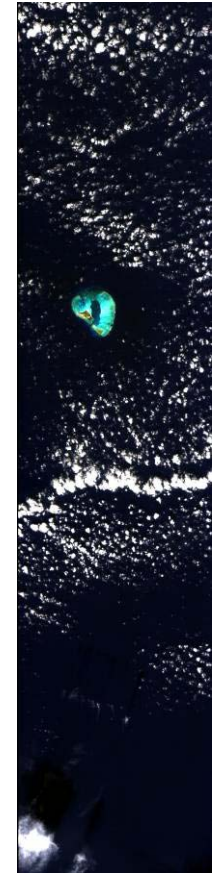
Florida Keys, over Key Largo, Sept. 27, 2009. Orientation is from SW at bottom to NE at top.



Sahara Desert over Egypt, Sept. 27, 2009. Orientation is from SW at bottom to NE at top.



Taken over the Bahamas, Oct. 2, 2009. Orientation is from NW at top to SE at bottom.



Gem of the Pacific. Midway Island, Sept. 27, 2009. Orientation is from NW at top to SE at bottom.

Spectral and Radiometrical Calibrations (Smear + 2nd Order Light Correction) Have Been Conducted to the HICO Data

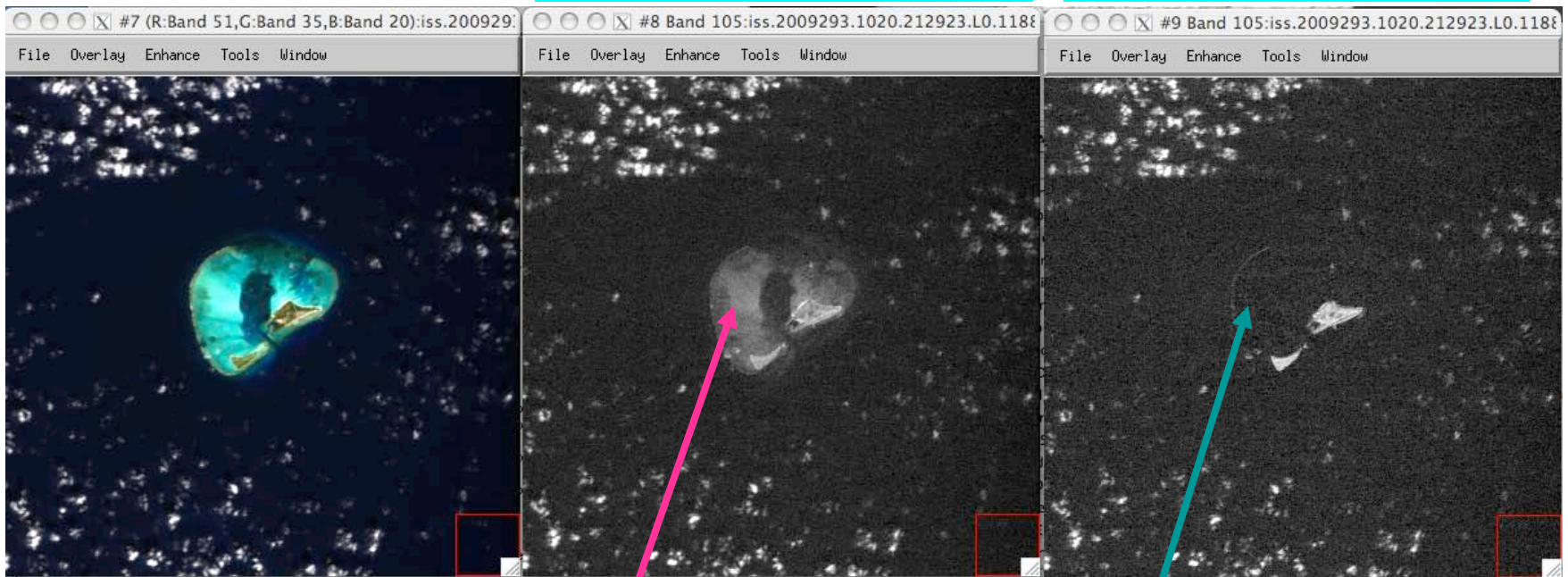
Here, we illustrate the results of an empirical technique for correction of 2nd order light effect using shallow underwater features

HICO Images Over the Midway Island in the Pacific Ocean

RGB image

Before 2nd order correction
(Band 105, 0.95 μm)

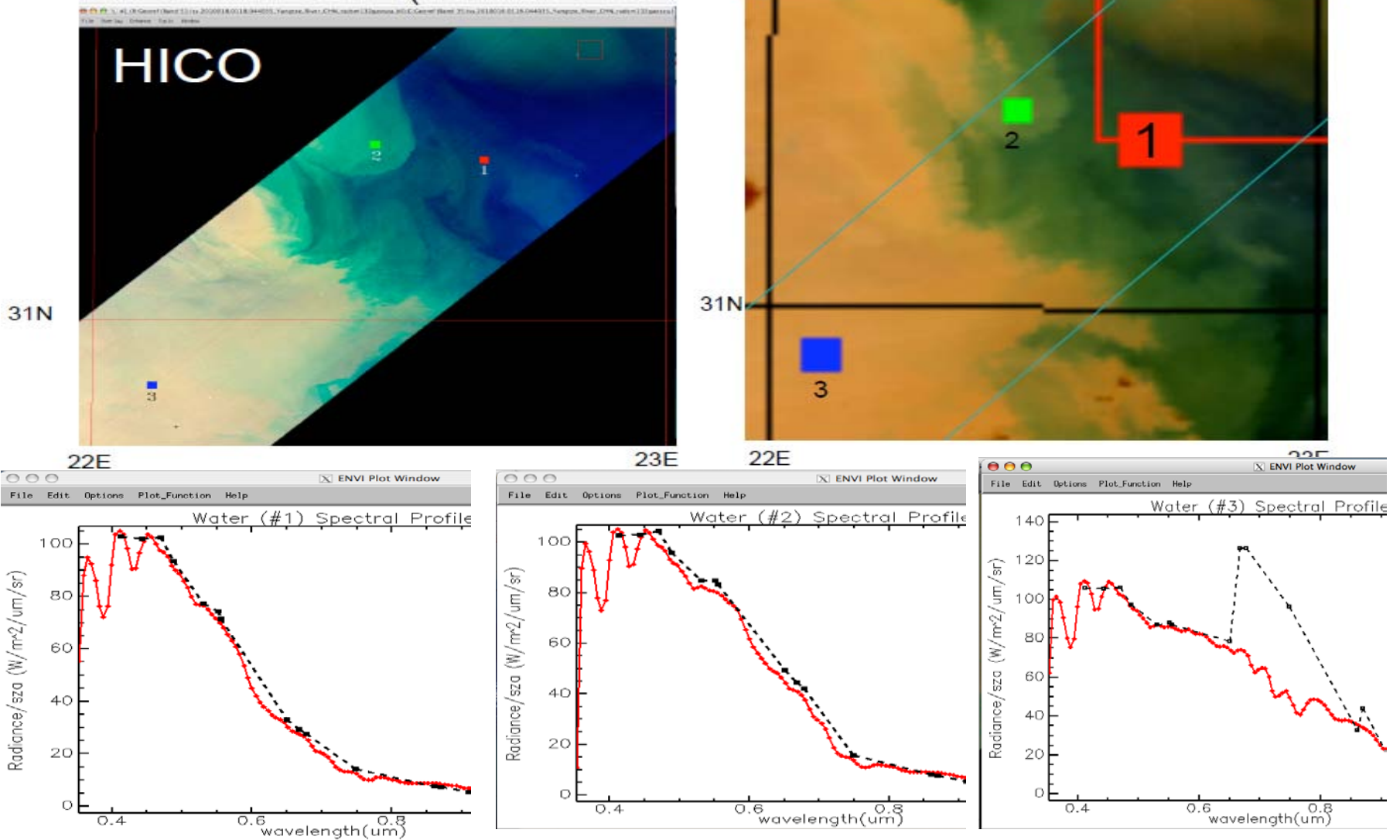
After 2nd order correction
(Band 105, 0.95 μm)



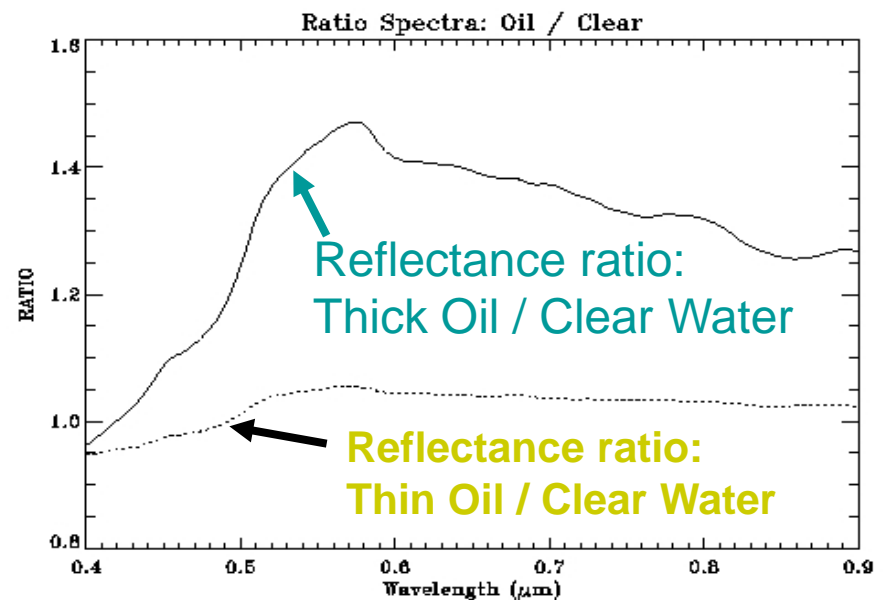
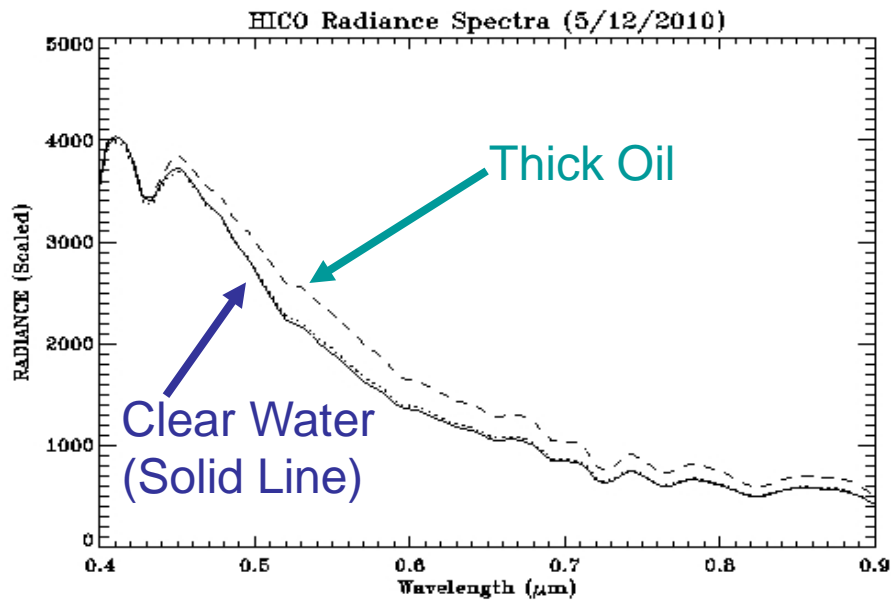
The bright features result from the 2nd order light of a visible channel

The bright features are removed

- Co-located HICO and MODIS Data Acquired Over Desert Areas Were Used to Adjust the HICO Gain Changes (from pre-launch lab-calibrations).
- After such adjustments, the radiances of HICO and MODIS data acquired over other surfaces, such as waters, agreed quite well.



HICO Image Over The Gulf of Mexico (Oil Spill, 5/12/2010)



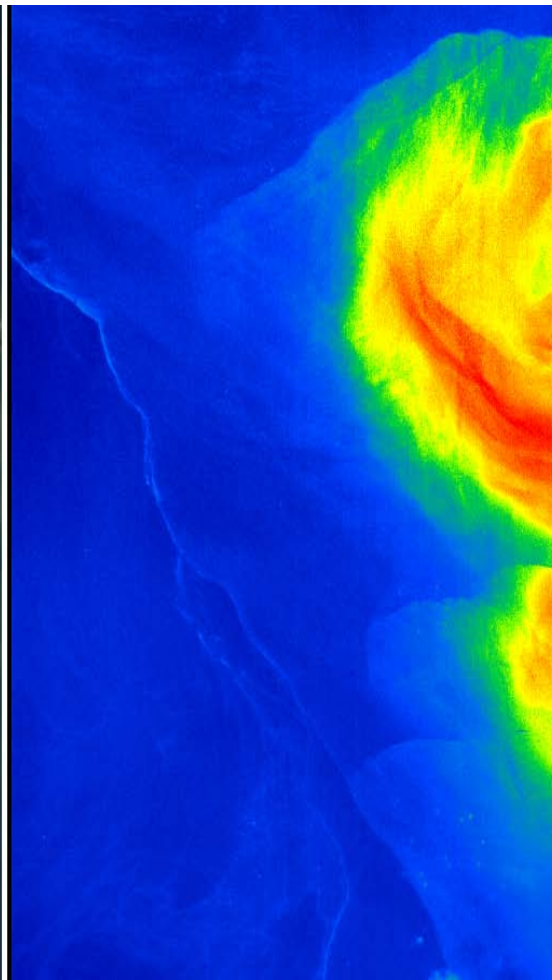
HICO RGB Image Over Gulf of Mexico, Chlorophyll & Kd_490 Images (5/24/2010)

RGB



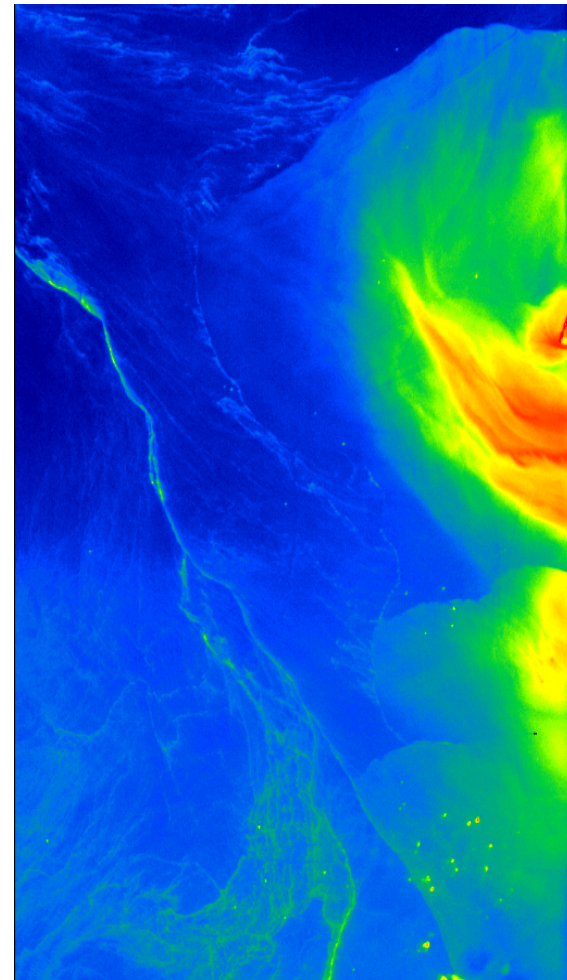
Chl

(mg/m³)



Kd_490

(m⁻¹)



HICO RGB Image Over Gulf of California, Chlorophyll & Kd_490 Images

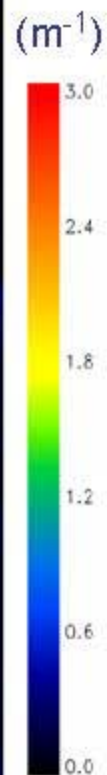
HICO (2009335.1201.155713), Gulf_of_California
RGB



Chlorophyll-a

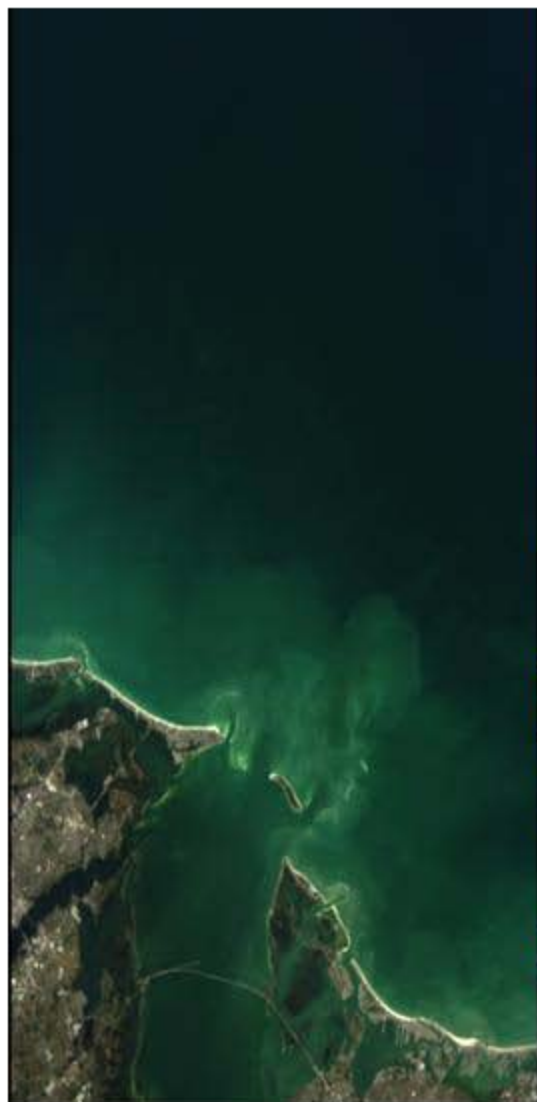


K_a(490)_comb



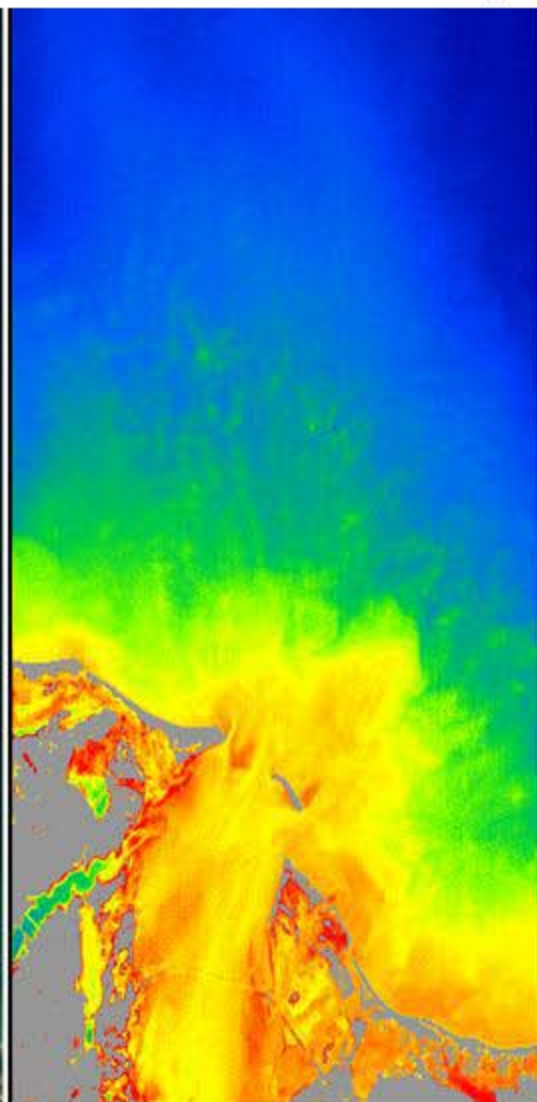
HICO RGB Image Over Tampa Bay, Chlorophyll & Kd_490 Images

RGB



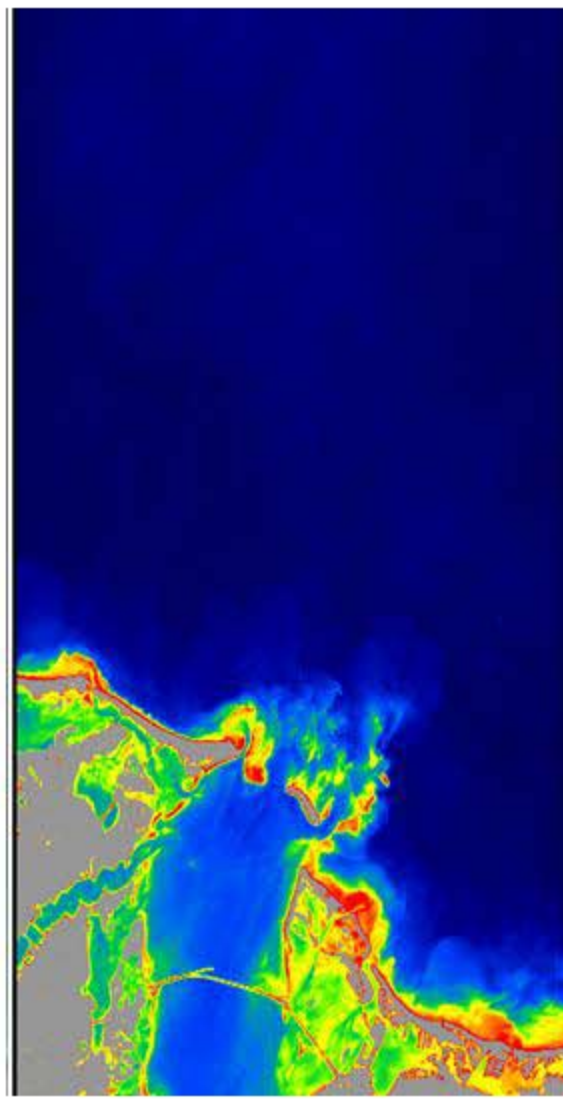
Chl

(mg/m³)



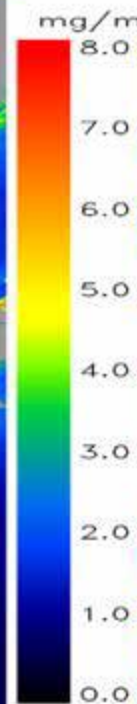
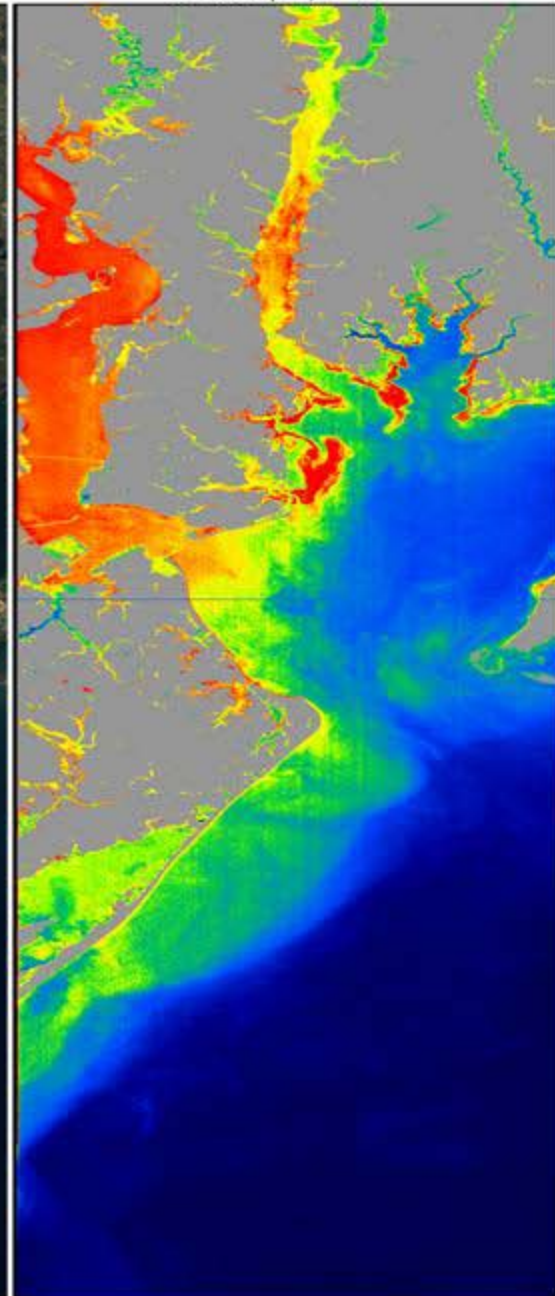
Kd_490

(m⁻¹)

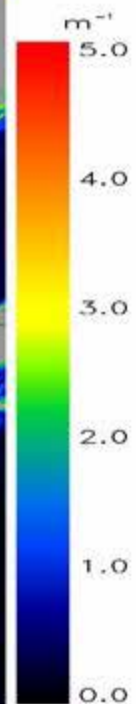
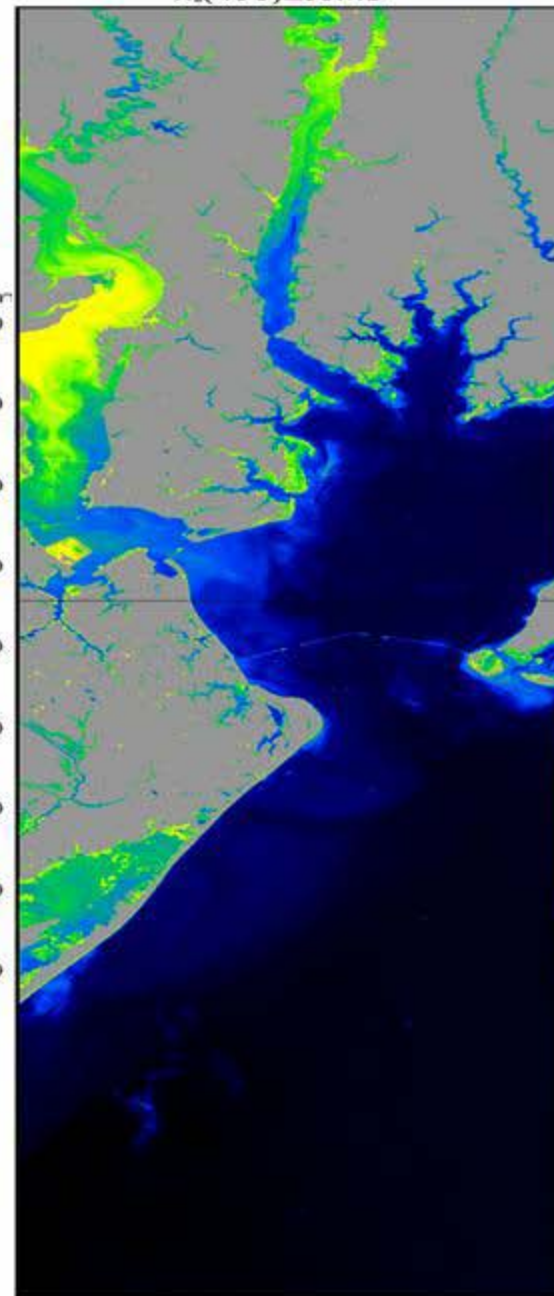


HICO RGB Image Over Chesapeake Bay, Chlorophyll & Kd_490 Images

HICO (2010091.0401.194053), Chesapeake_CapeHenr
RGB



K_d(490)_comb

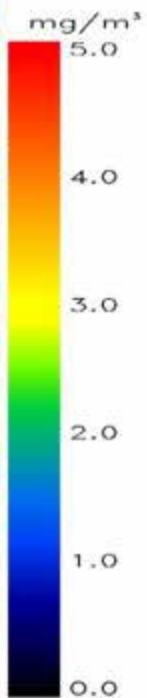
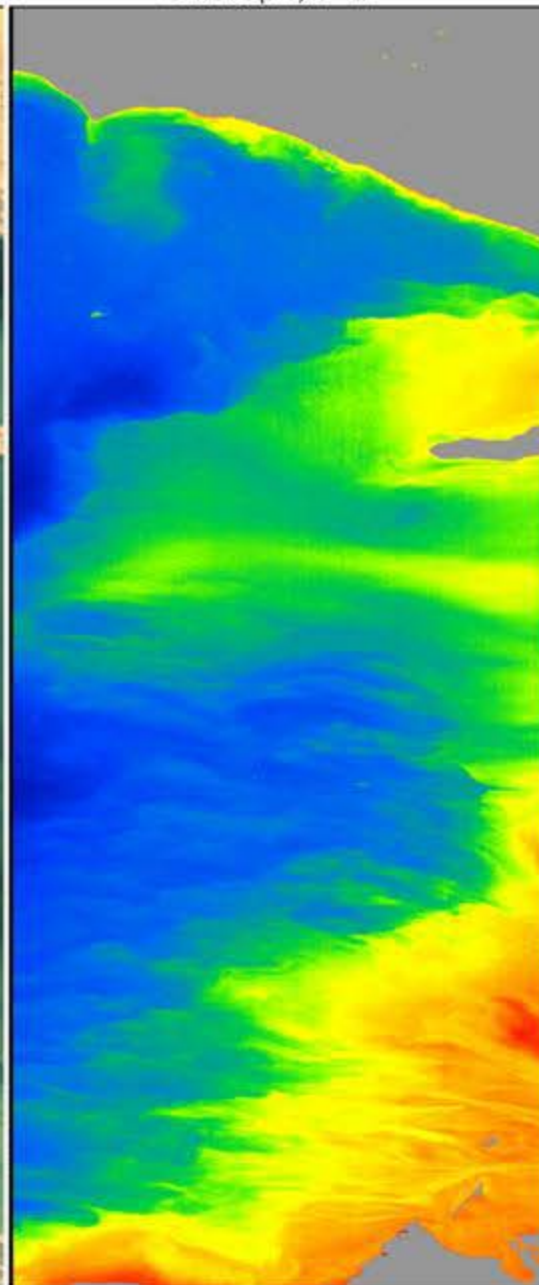


HICO RGB Image Over Persian Gulf, Chlorophyll & Kd_490 Images

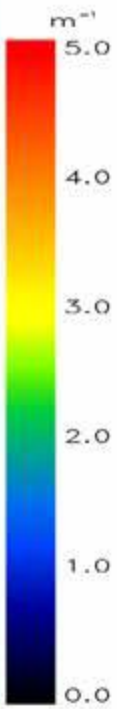
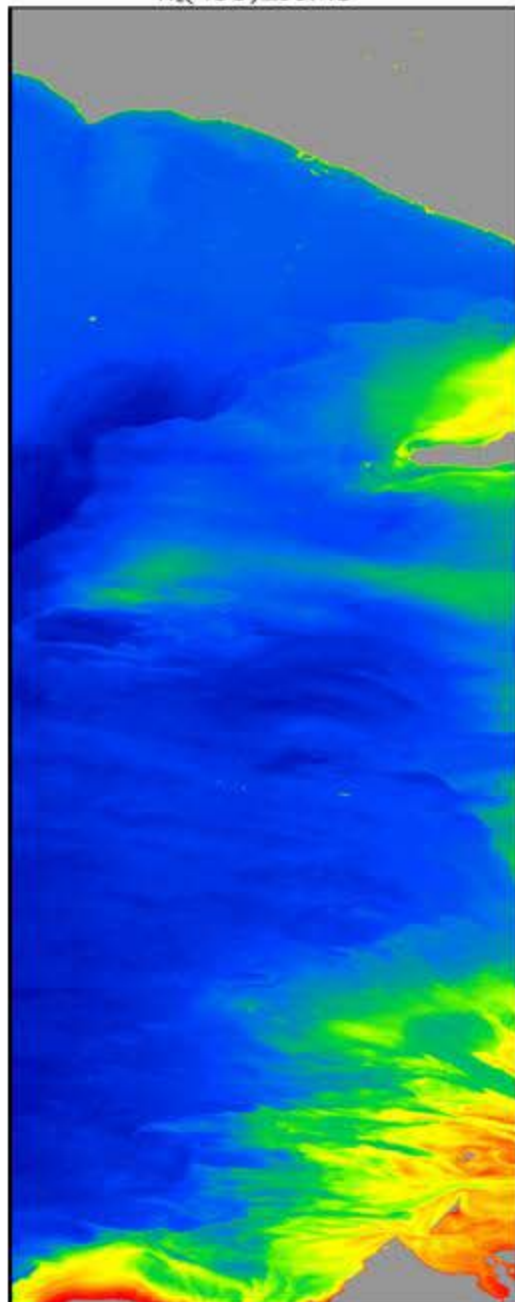
HICO (2010206.0725.045136), Persian_Gulf
RGB



Chlorophyll-a



K_d(490)_comb

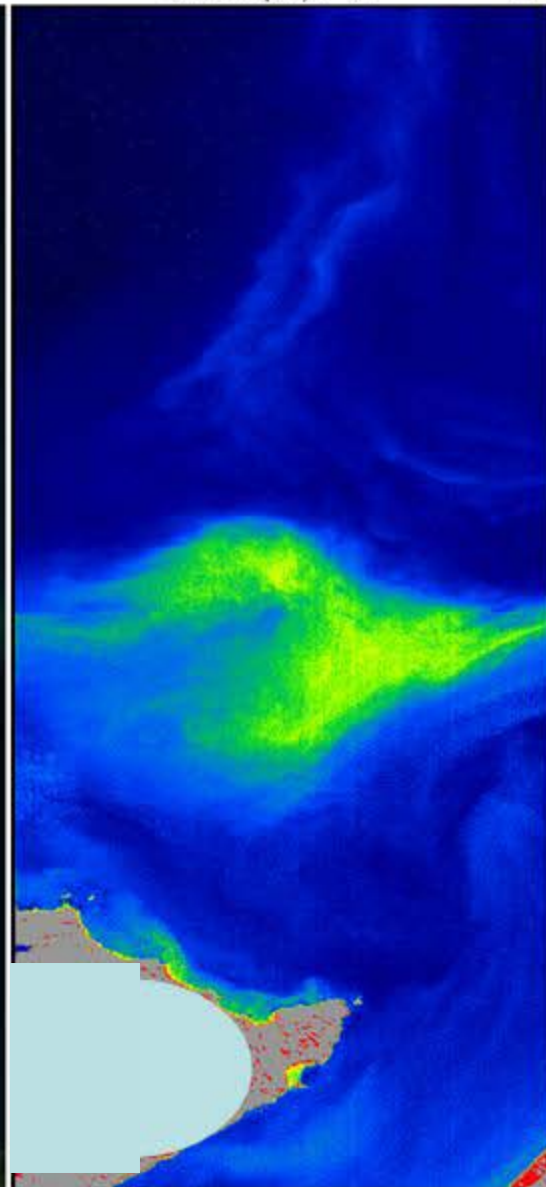


HICO RGB Image Over Olympic Beaches (WA), Chlorophyll & Kd_490 Images (7/9/2010)

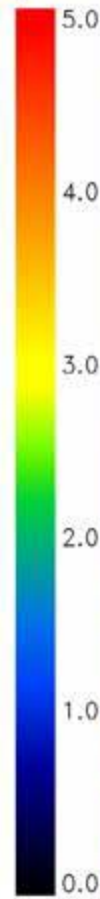
HICO (2010190.0709.012442), Olympic_Beaches_WA
RGB



Chlorophyll-a



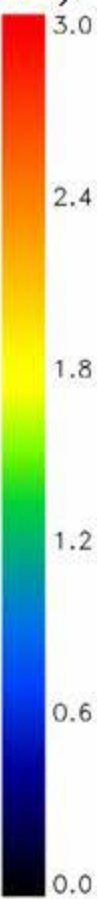
(mg/m³)



K_d(490)_comb



(m⁻¹)

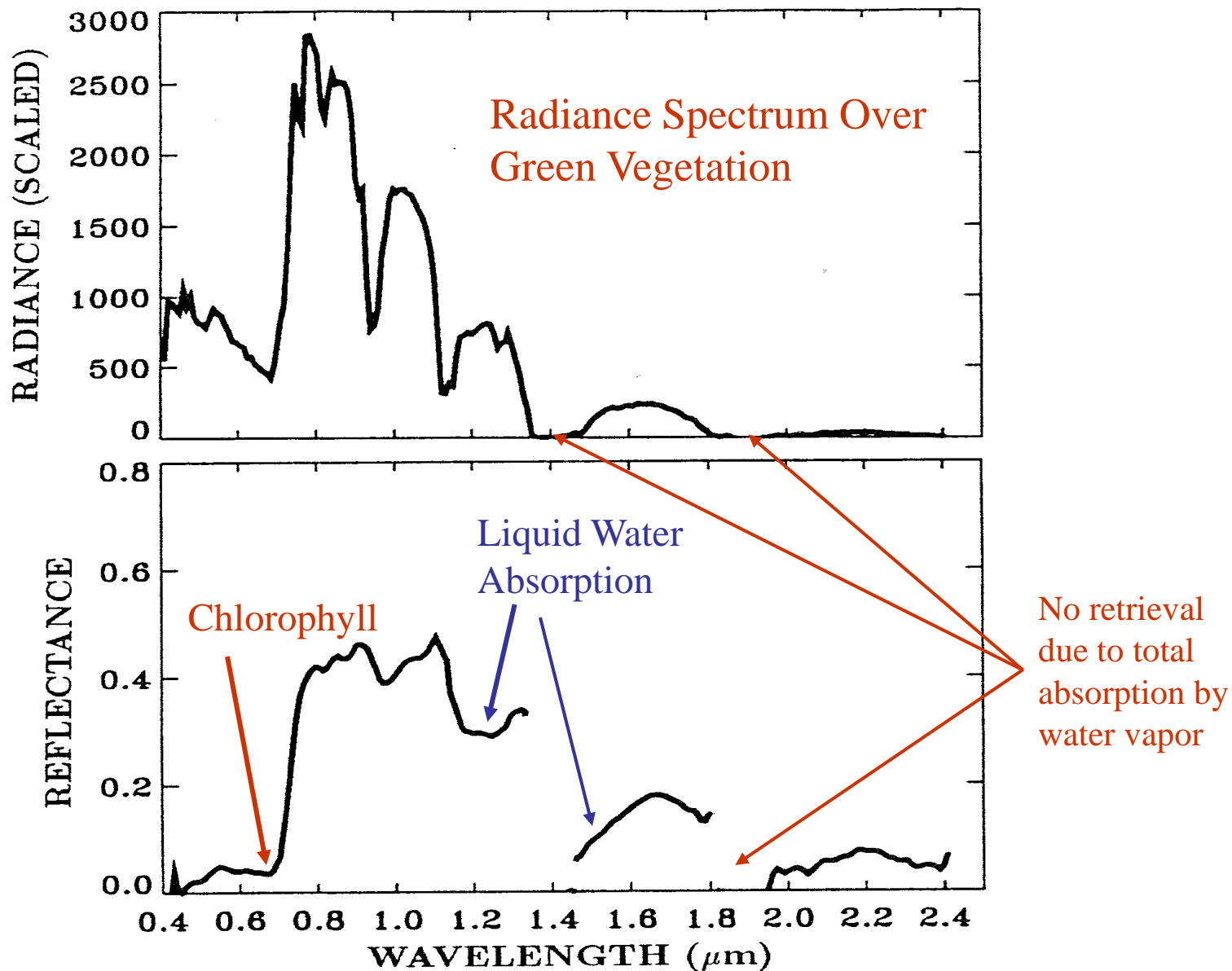


Summary

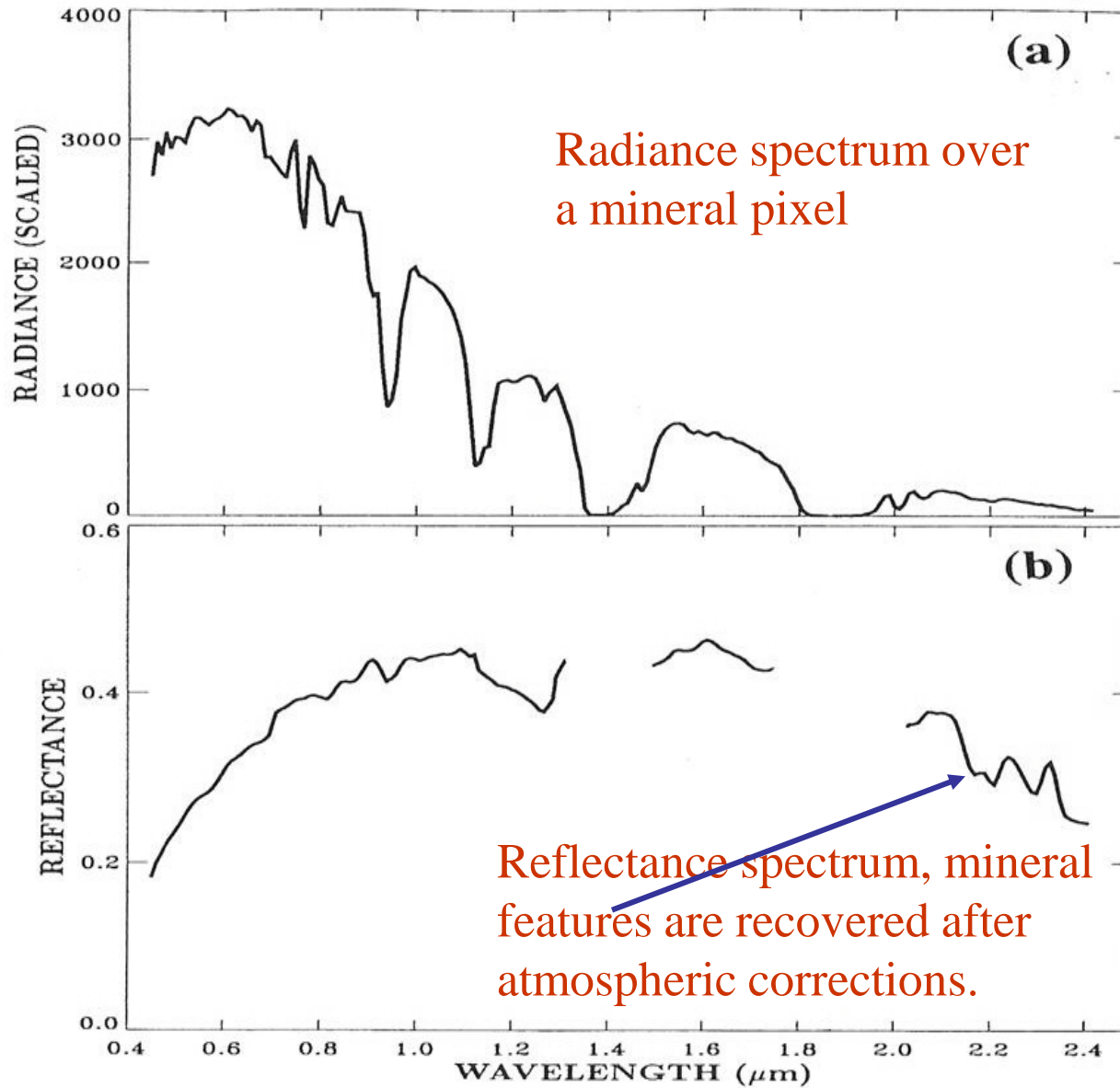
- At present, both the land and ocean version of the algorithms work reasonably well under typical atmospheric conditions.
- However, in the presence of absorbing aerosols, the model tends to overestimate the atmospheric contribution to the upwelling radiance, resulting in inferred surface reflectances which are biased low (even negative) in the blue region of the spectrum. Problem has been most prevalent in:
 - US east coastal areas in summer months
 - Desert regions
- Upgrades to the atmospheric correction algorithms are needed, particularly in view of major advances in aerosol models. Specific upgrades include:
 - Incorporation of absorbing aerosol models
 - Incorporation of UV channels (380 nm, 400 nm)

Backup Slides

SAMPLE REFLECTANCE RETRIEVALS WITH ATREM



SAMPLE REFLECTANCE RETRIEVALS OVER MINERAL



Examples of Cirrus Detection & Corrections

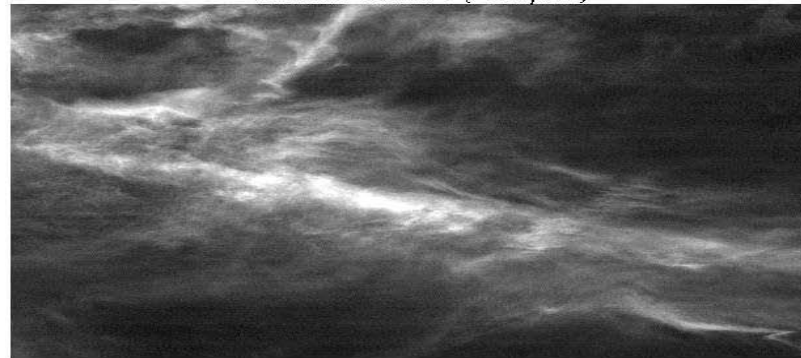
AVIRIS data acquired over Bowie, MD in summer 1997



CIRRUS IMAGE ($1.38\mu\text{m}$)



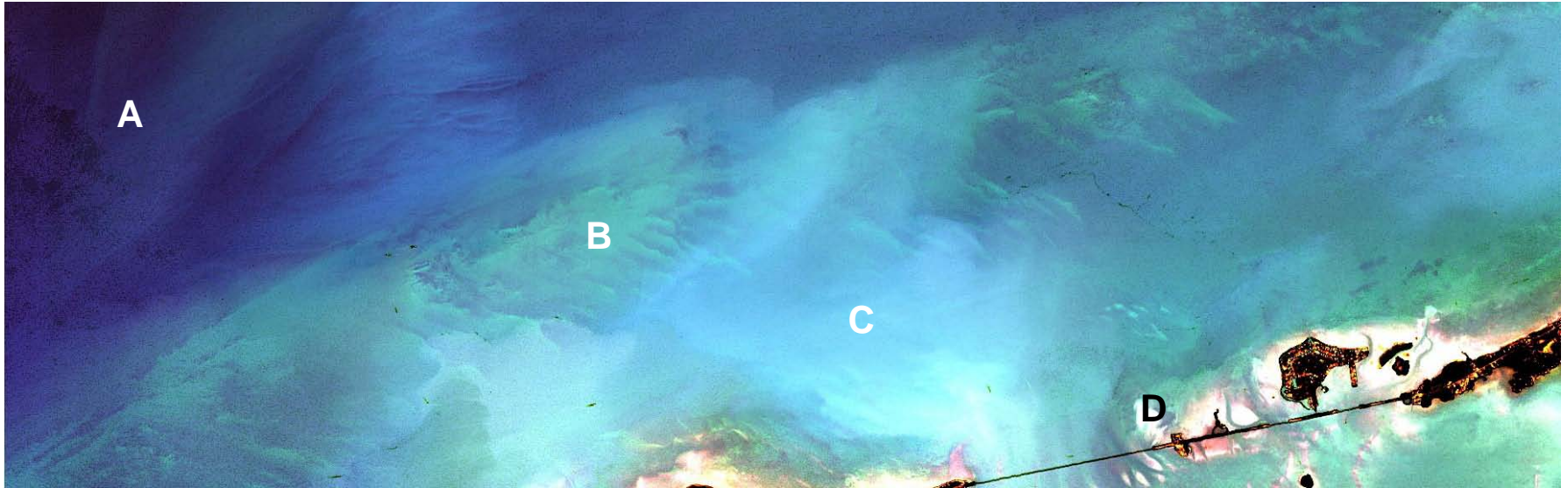
Hwy 50



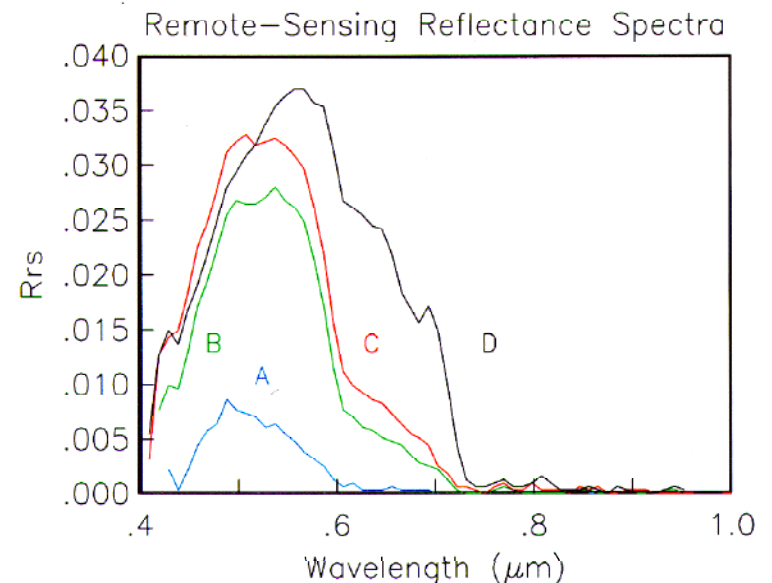
CIRRUS-CORRECTED IMAGE



An Example of Ocean Atmospheric Correction Including Surface Glint Correction

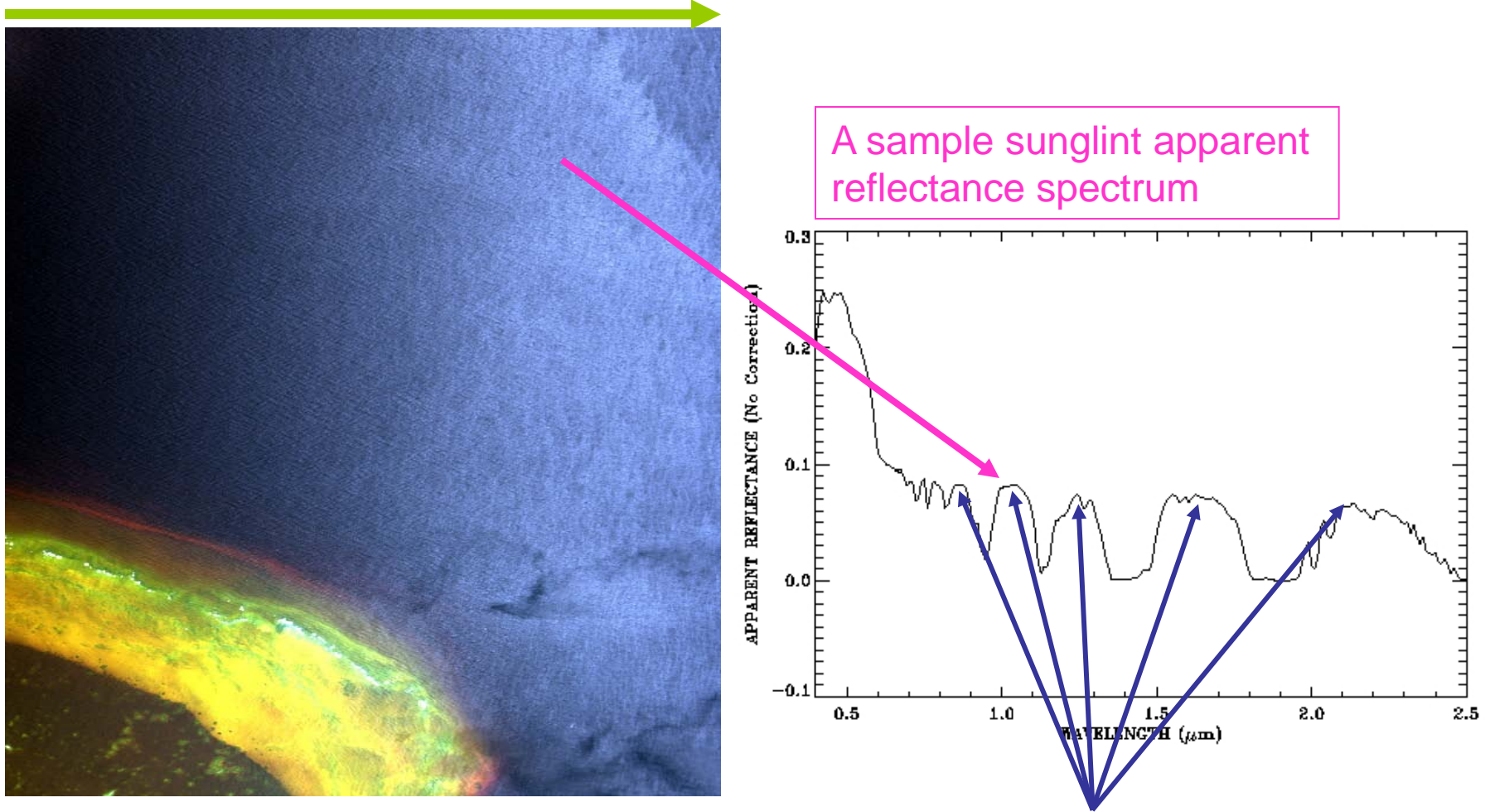


AVIRIS data were atmospherically corrected for ocean scenes. The data are corrected for skylight reflected off the sea surface. It is assumed that the water leaving radiance is 0 for wavelengths greater than 1.0 micron. Note how all of the spectra are 0 past 0.82 micron. (B.-C. Gao, M. J. Montes, Z. Ahmad, and C. O. Davis, *Appl. Opt.* 39, 887-896, 2000.)



Sunglint Effect Removal With An Empirical Technique

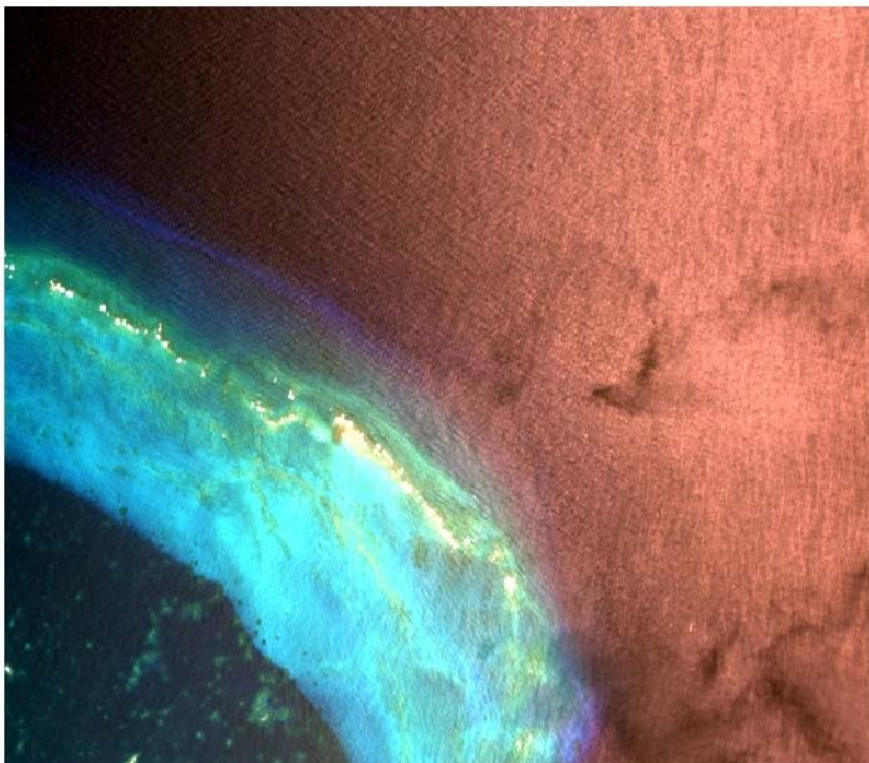
Sunglint effect becomes stronger from left to right in an AVIRIS image. Individual wave facets are observed in the high spatial resolution AVIRIS image (20 m). It is not possible to use Cox & Munk model to predict sun glint effects in this case.



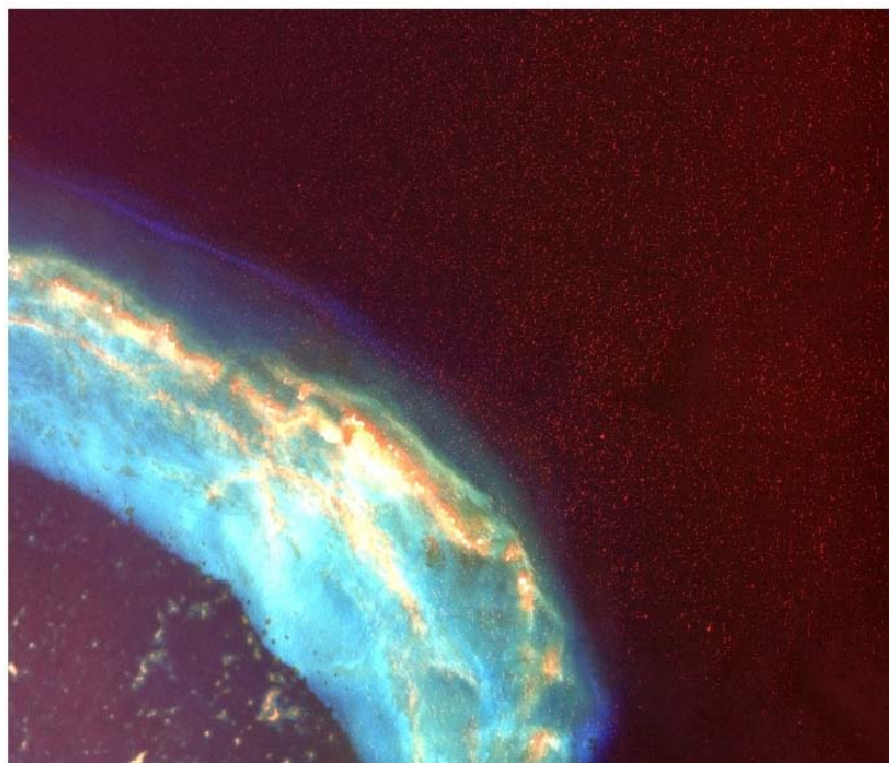
The sunglint reflectances for atmospheric window channels above 0.8 micron are almost constant. The empirical technique = ATREM (Land) reflectance minus 1.04 micron reflectance value on the pixel by pixel basis.

Images Before and After The Empirical Sunglint Correction

Before



After

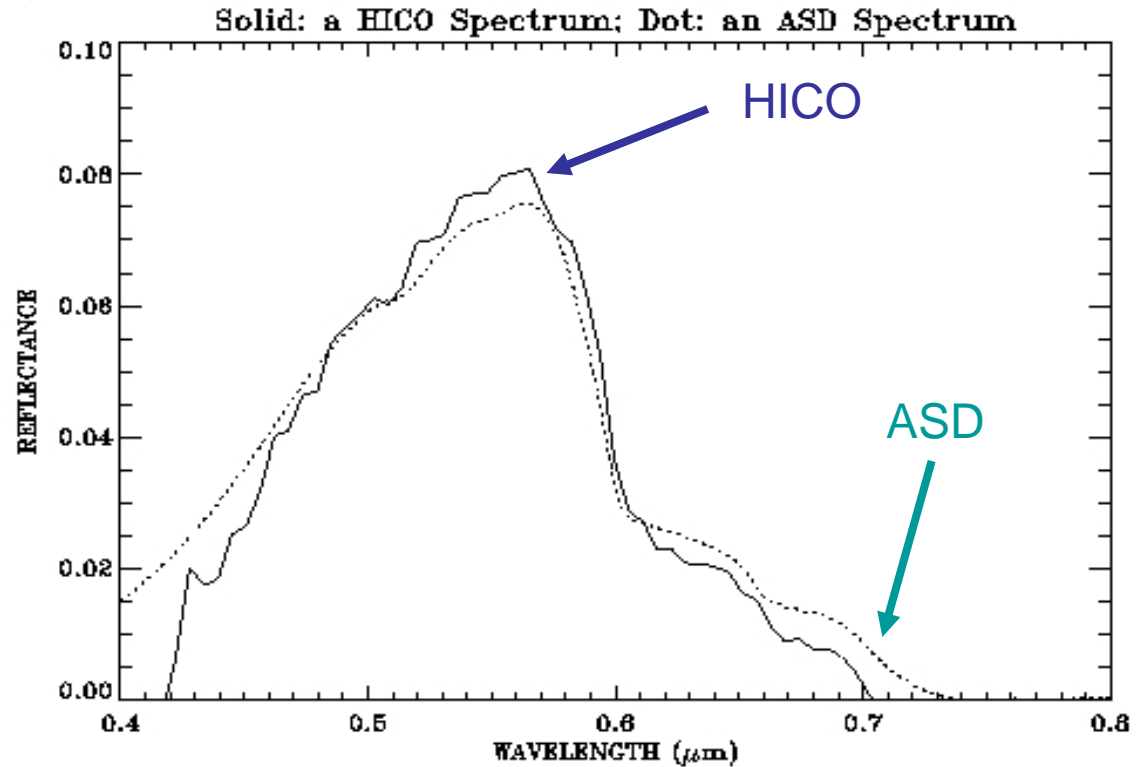


The image at right demonstrates that, after the empirical correction, the sunglint effects are mostly removed. The “contiguous” spatial features in the middle bottom portions of the image are seen much better. However, minor noise effects are seen in areas without bottom reflection.

HICO RGB Image & Sample Spectra of Florida Keys



Examples of an ASD Spectrum and a Water Leaving Reflectance Spectrum Retrieved From HICO Data Over Florida Keys



Please note that the shapes of the two spectra in the 0.45 – 0.8 micron wavelength Interval are very similar. The two spectra are not measured over the same time, nor over the same spatial location.

Spectral and Radiometrical Calibrations (Smear + 2nd Order Light Correction) Have Been Conducted to the HICO Data

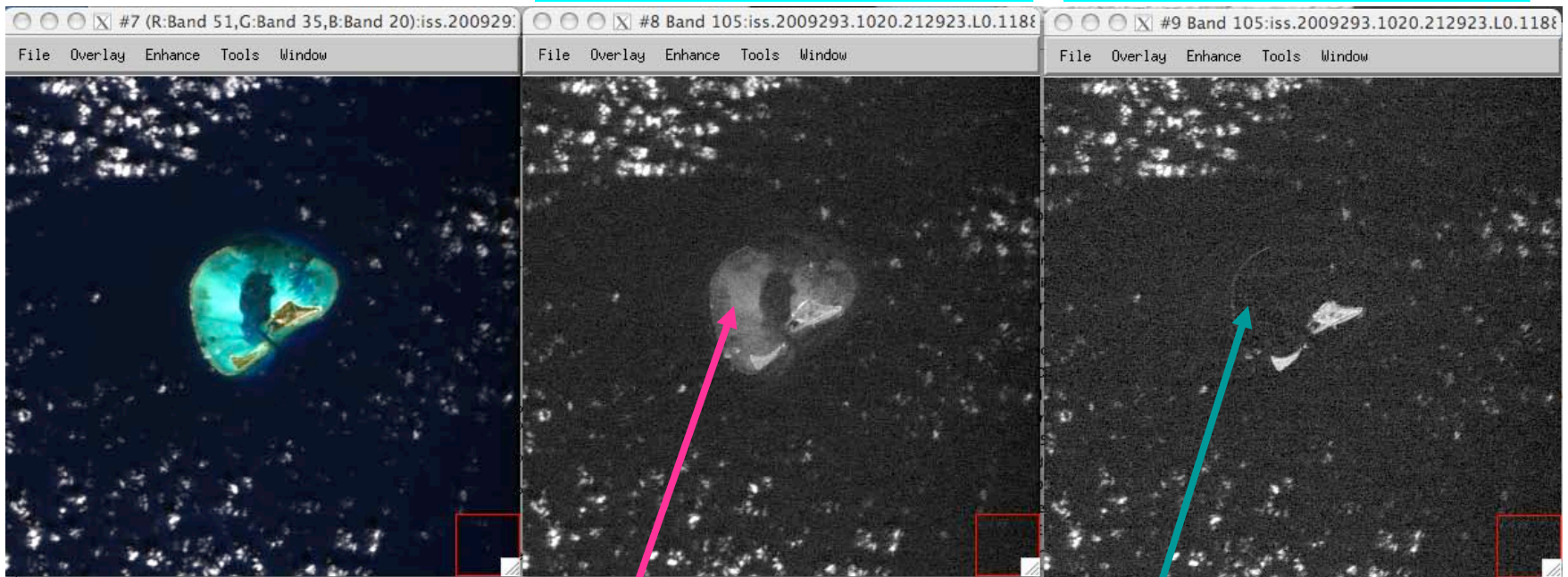
Here, we illustrate the results of an empirical technique for correction of 2nd order light effect using shallow underwater features

HICO Images Over the Midway Island in the Pacific Ocean

RGB image

Before 2nd order correction
(Band 105, 0.95 μm)

After 2nd order correction
(Band 105, 0.95 μm)



The bright features result from the 2nd order light of a visible channel

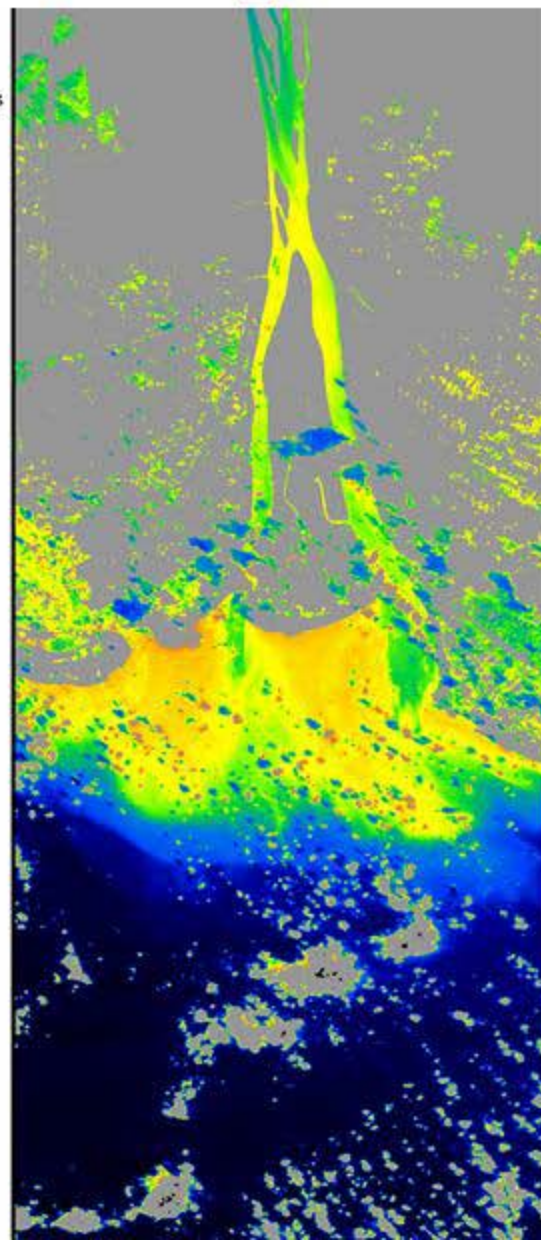
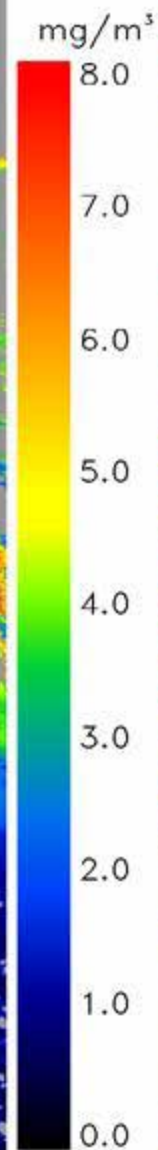
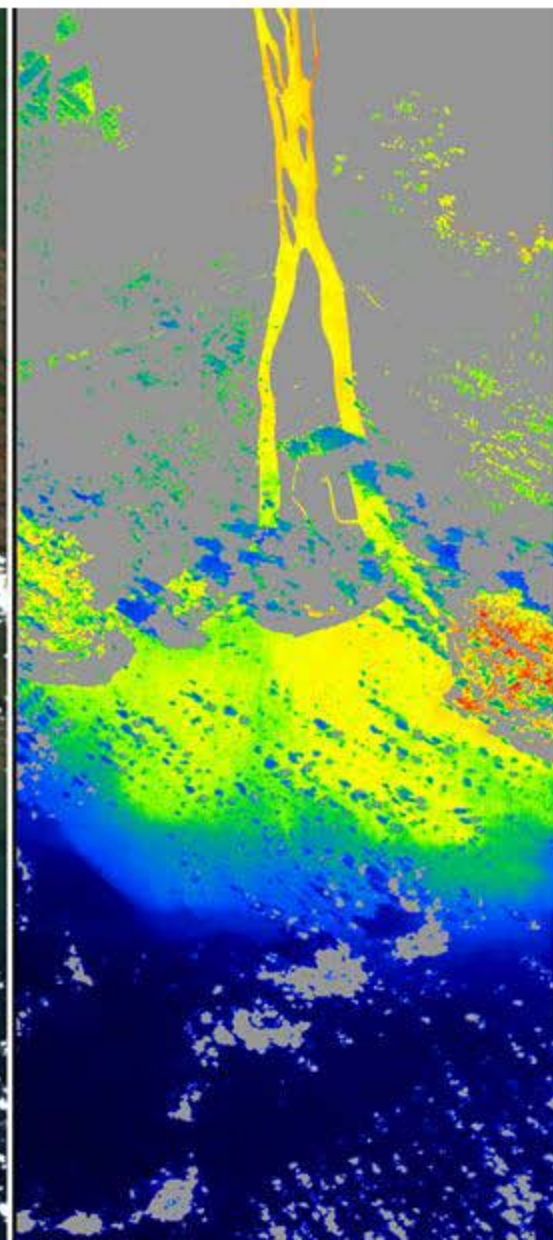
The bright features are removed

HICO RGB Image Over Mekong Delta, Chlorophyll & Kd_490 Images

RGB

Chl

Kd_490

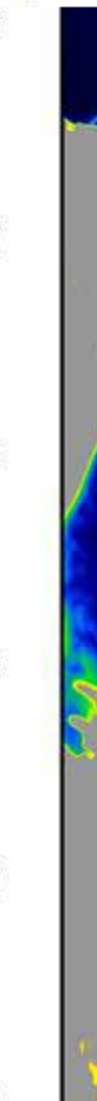
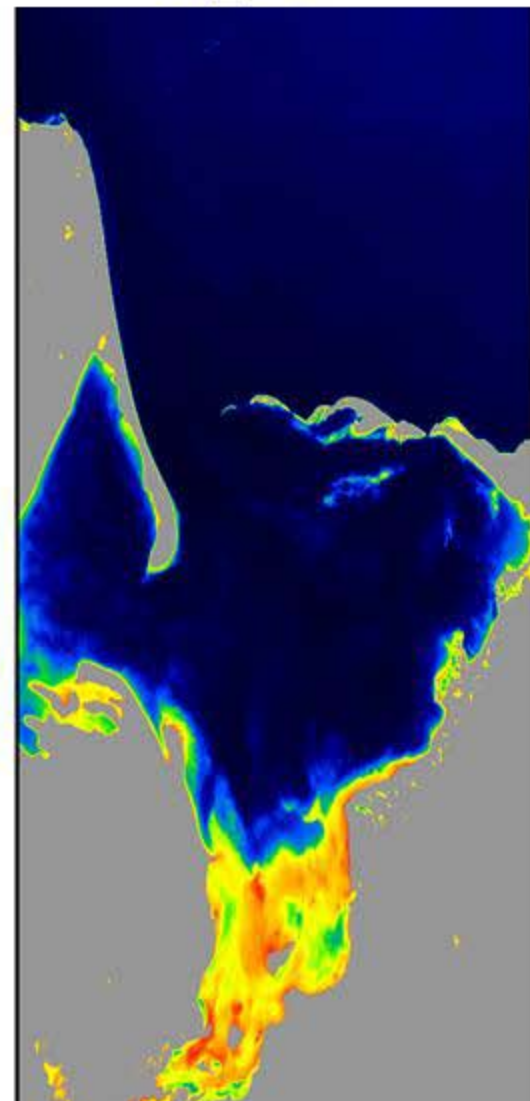
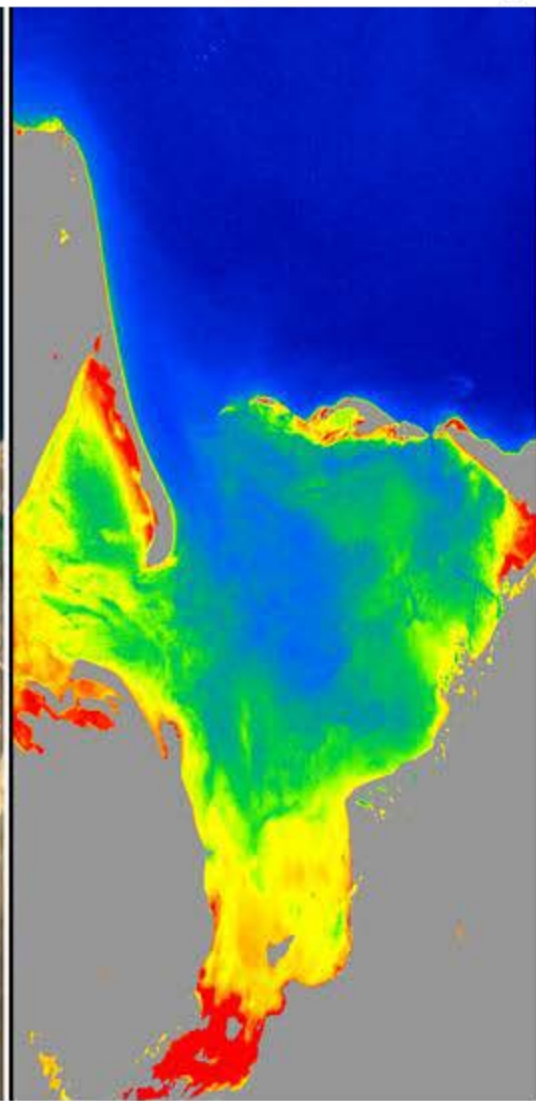


HICO RGB Image Over SE Caspian Sea, Chlorophyll & Kd_490 Images
(5/9/2010)

RGB

Chl (mg/m³)

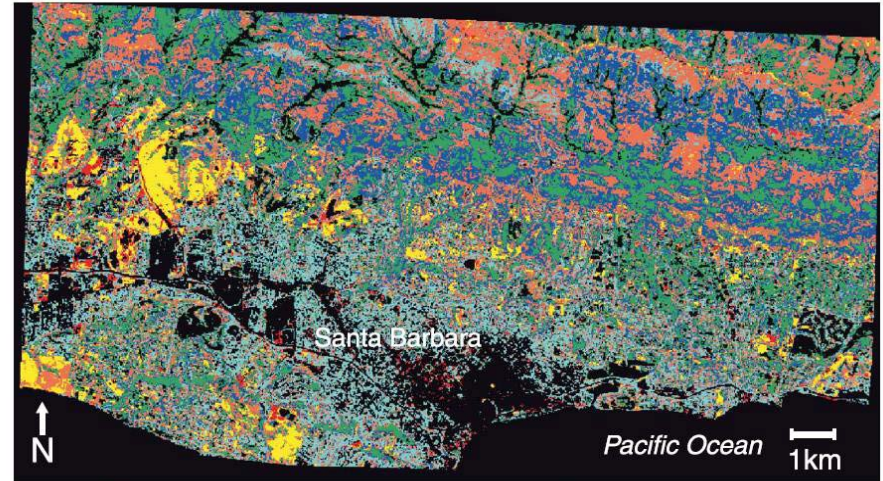
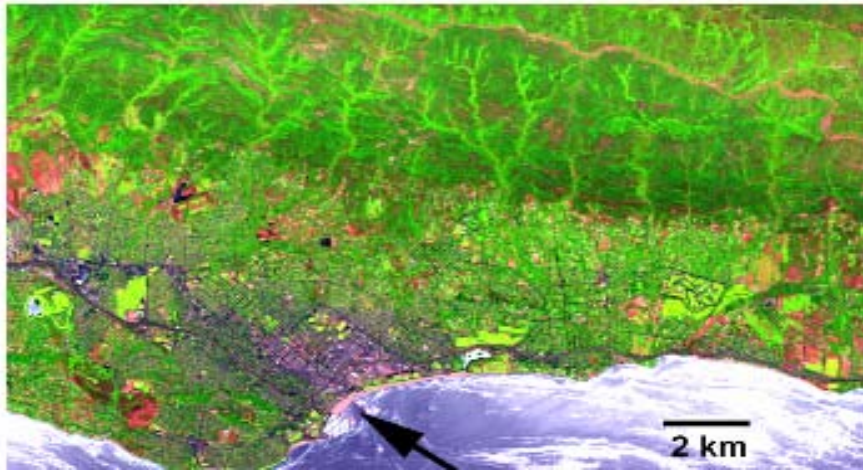
Kd_490 (m⁻¹)



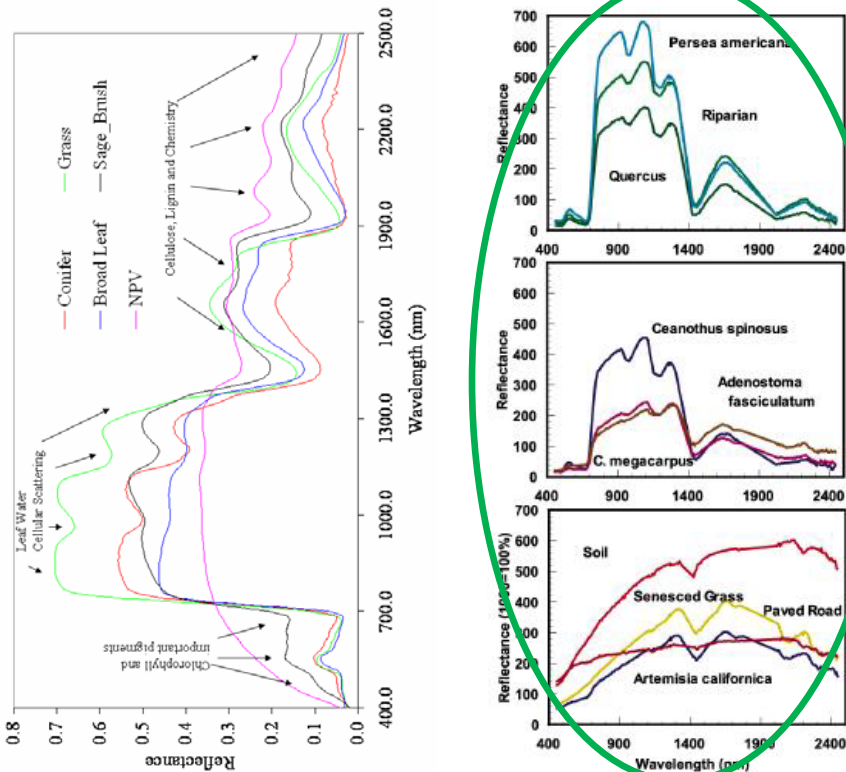
Vegetation Functional Type Analysis, Santa Barbara, CA

Dar Roberts, et al, UCSB

MESMA Species Type 90% accurate



- *Adenostoma fasciculatum*
- *Ceanothus megacarpus*
- *Arctostaphylos* spp.
- *Quercus agrifolia*
- Grass
- Soil



Species Fractional Cover

